Marine Pollution Bulletin 209 (2024) 117220

Contents lists available at ScienceDirect

Marine Pollution Bulletin

journal homepage: www.elsevier.com/locate/marpolbul

Apportioning sources of natural and anthropogenic organic matter in sediment from Lake Shihwa: An integrated approach using molecular ratios and compound-specific stable-isotope analysis

Rincheon Jeon [a,1], Seung-Hee Kim [b], Dong-Hun Lee [c,*], Yusang Cho [a], Youngnam Kim [d], Seongjin Hong [d], Kyung-Hoon Shin [a,*]

[a] Department of Marine Sciences and Convergent Technology, Hanyang University, Ansan 15588, Republic of Korea
[b] Institute of Sustainable Earth and Environmental Dynamics, Pukyong National University, 365 Sinseon-ro, Nam-gu, Busan 48547, Republic of Korea
[c] Division of Earth and Environmental System Sciences, Pukyong National University, 45, Yongso-ro, Busan 48513, Republic of Korea
[d] Department of Earth, Environmental & Space Sciences, Chungnam National University, Daejeon 34134, Republic of Korea

ARTICLE INFO

Keywords:
Organic matter
n-Alkanes
Polycyclic aromatic hydrocarbons (PAHs)
Compound specific isotope analysis
Bayesian mixing model
Lake Shihwa

ABSTRACT

We tested an integrated multi-isotopic analysis framework to quantitatively estimate anthropogenic organic matter (OM) loads in different land-use types of a watershed (Lake Shihwa, South Korea). The isotopic signatures of increased bulk-element abundances in urban areas and industrial complexes may reflect the mixed contributions of natural and anthropogenic sources. Together with the predominant abundance of *n*-alkanes and polycyclic aromatic hydrocarbons at both boundaries, specific indices derived from their abundance may be indicative of mixed contributions from terrestrial plants, petroleum, and combustion deposited through various pathways (e.g., atmospheric deposition, outfall pipes, and surface runoff). Based on these properties, compound isotopic signatures ($\delta^{13}C_{C27+C29+C31}$, $\delta^{13}C_{Fl}$, $\delta^{13}C_{Pyr}$, $\delta^{13}C_{BaA+Chry}$, $\delta^{13}C_{IcdP}$, $\delta^{13}C_{BghiP}$,) for both land-use types may provide significant evidence of an increase in anthropogenic derived-OM loads (> 90 %) in Lake Shihwa. This approach suggests that total organic carbon–weighted source apportionments can provide useful quantitative estimates of OM loads within complex river systems.

1. Introduction

Coastal regions are hot spots of organic matter (OM) sedimentation, accounting for 80–90 % of the carbon burial in the global ocean (Hedges and Keil, 1995; Bauer et al., 2013). The transport of OM from land to aquatic systems, such as rivers and lakes, plays a critical role in sustaining aquatic ecosystems (Bouwman et al., 2013; Vörösmarty et al., 2010; Walling, 2006). Together with physical dynamics such as mixing, processing, and transportation, a substantial amount of OM exchanged between the terrestrial and marine realms has been continuously preserved in the coastal sediment layers due to the inputs of terrestrial materials, anthropogenic contamination, and marine organisms (Hedges and Oades, 1997; Bianchi et al., 2002; Ogrinc et al., 2005; Li et al., 2017; Chen et al., 2021). As these aspects, the biogeochemical role of OM is important for maintaining the ecological health of aquatic systems by contributing to nutrient cycling, and providing an essential energy source for aquatic food webs through microbial decomposition and energy transfer across trophic levels (Hedges and Keil, 1995). However, human activities can alter the structure and the function of aquatic ecosystems, ultimately decreasing biodiversity and increasing eutrophication, algal blooms, and the bioaccumulation of contaminants (Kelly et al., 2007; Newbold et al., 2015; Smith et al., 1999; Van der Oost et al., 2003). The precise identification of natural and anthropogenic OM sources for aquatic ecosystems is therefore necessary to evaluate the potential impacts on water quality deterioration and bioaccumulation in aquatic environments and surrounding land-use practices. These insights can provide a wealth of information on how to manage transfers that degrade water quality and threaten water security.

The bulk-element contents (e.g., carbon and nitrogen) and their stable isotopic compositions ($\delta^{13}C$ and $\delta^{15}N$) are popular tools for tracking the sources of various forms of OM (Gao et al., 2012; Hedges et al., 1988; Sarma et al., 2014). Bulk analysis was first performed on

* Corresponding authors.
E-mail addresses: ldh301@pknu.ac.kr (D.-H. Lee), shinkh@hanyang.ac.kr (K.-H. Shin).
[1] Present address: Underwater Survey Technology 21, Incheon, Republic of Korea.

https://doi.org/10.1016/j.marpolbul.2024.117220
Received 9 September 2024; Received in revised form 21 October 2024; Accepted 27 October 2024
Available online 5 November 2024

natural samples to identify the sources and transformation processes of OM (Fry and Sherr, 1989). Although previous studies demonstrated the ability of stable-isotope ratios to distinguish between allochthonous and autochthonous origins (Ramaswamy et al., 2008; Saintilan et al., 2013), they suffer from intrinsic limitations for source determination in complex watersheds (Canuel et al., 1997; Cloern et al., 2002; Hu et al., 2006; Poynter and Eglinton, 1991). As advanced techniques, the developed approaches such as ^{11}B, $^{15}N\text{-}NO_3$, $^{18}O\text{-}NO_3$, and $^{15}N\text{-}NH_4$, provide more precise identification of anthropogenic sources in environmental samples (Divers et al., 2014; Martinelli et al., 2018; Ryu et al., 2021). These methods offer a more refined understanding of pollution sources, particularly in cases where traditional bulk isotopic applications are inadequate (Ryu et al., 2021; Kim et al., 2023). Meanwhile, a molecular biomarker can provide more detailed insights for identifying OM origins and related biogeochemical processes, aiding in the interpretation of environmental changes (Bosch et al., 2015; Bourbonniere and Meyers, 1996; Meyers, 1997; Zhang et al., 2019). In this regard, hydrocarbons which are ubiquitously present in various types of OM sources (e.g. soils, sediments, organisms, and atmospheric dust), are degraded more slowly than bulk OMs and other lipid classes (e.g. fatty acids and alcohols), making them valuable indicators in complex system (Meyers, 2003; Wang et al., 2013; Pedrosa-Pàmies et al., 2015). Among them, aliphatic (*n*-alkanes) and polycyclic aromatic hydrocarbons (PAHs) are representative molecular markers of OM derived from natural and anthropogenic sources, such as fungi, bacteria, algae, biomass and/or fossil-fuel combustion, and petroleum residue (Bush and McInerney, 2013; Stogiannidis and Laane, 2015; Wakeham et al., 1980; Zhang et al., 2022). Source-recognition ratios based on their abundances are reliable indicators for tracing OM sources in complex aquatic systems surrounded by various types of land use (Colombo et al., 1989; Medeiros et al., 2005; Venturini et al., 2015; Yunker et al., 2002; Zhang et al., 2023). However, with respect to quantitatively determining OM sources in a complex aquatic system, the spatial abundance of both *n*-alkanes and PAHs can be influenced by physical processes (particle transport and phase transfer) and chemical and microbial processes (Galarneau, 2008; Liu et al., 2021; Wentzel et al., 2007). Using a more recently developed and more advanced technique (compound-specific isotope analysis [CSIA]), the isotopic signature of aliphatic or aromatic hydrocarbons has the potential to facilitate source-tracing within coastal and lake sediment, including those of OM (Canuel et al., 1997; Cooper et al., 2015; Gschwend and Hites, 1981; Li et al., 2021; Maletić et al., 2019). However, precise quantitative assessment of OM origins remains challenging in aquatic systems in which heterogeneous OM transport occurs.

In this study, we hypothesized that molecular ratios and CSIA can (1) improve the accuracy of OM source appointment and (2) distinguish between OM loads of natural and anthropogenic origins. To test our hypothesis, we performed a case study in Lake Shihwa, where the land use varies in the surrounding watershed (e.g., urban, industrial, and rural areas). At these sites, environmental qualities (e.g., water and sediment quality and biodiversity) are threatened by large inputs from anthropogenic sources (e.g., trace metals, persistent organic pollutants, and petrochemical spills) (Khim et al., 1999; Yoo et al., 2008; Lee et al., 2014; Moon et al., 2012). Environmental qualities (e.g., biological oxygen demand: 6.5–69.9 ppm; chemical oxygen demand: 11.1–103.2 ppm; heavy metals: 1.14–511 ppb) have deteriorated dramatically in the lake since a sea dike was constructed in 1994 (Ministry of maritime affairs and fisheries (MOMAF), 2011; Ra et al., 2011). Substantial increases in PAHs, styrene oligomers, and alkylphenols at Lake Shihwa have been traced to stormwater drainage pipes that carry pollutants from upland areas to creeks feeding into the lake (Hong et al., 2019; Lee et al., 2017b). Therefore, the main objectives of this study were to identify natural and anthropogenic sources of OM in different land-use types, and to constrain the discriminative contributions of these OM sources to Lake Shihwa sediment.

2. Materials and methods

2.1. Sampling

Surface sediment samples were collected during two sampling campaigns (July and December 2020) (Fig. 1). For this study, 35 sampling sites were selected within different land-use types (9 urban areas; 11 old industrial complexes; 4 new industrial complexes; 1, rural area; and 10 lake-sediment sites). Sediment samples were collected using Van Veen grab samplers. Creek surface sediment was collected using aluminum spoons. Both lake and creek surface sediment samples (from the uppermost 2 cm) were transferred to glass jars. All sediment samples were then freeze-dried and sieved (through 1 mm pores) and then ground using a mortar. The homogenized samples were stored at −20 °C prior to geochemical analysis.

2.2. Bulk-element analysis

The contents and isotopic compositions of total organic carbon (TOC; $\delta^{13}C_{TOC}$) and total nitrogen (TN; $\delta^{15}N_{TN}$) were analyzed using an elemental analyzer (Vario Select Elementar, Hesse, Germany) connected to an isotope-ratio mass spectrometry (VisION Elementar, Hesse, Germany). For TOC analysis, inorganic carbon in sediment samples was removed using 1 M HCl for 24 h under a fume hood, after which the acidified sediment was neutralized by washing it three times with deionized water (Kim et al., 2016). The isotopic composition was expressed by δ notation relative to Vienna Pee-Dee Belemnite and atmospheric N_2 for carbon and nitrogen, respectively. Instrumental checks were conducted using standard material IAEA-CH-3 (C = 44.4 wt%, $\delta^{13}C = -24.72$ ‰) and IAEA-N-1 ($N = 21.4$ wt%, $\delta^{15}N = 0.4$ ‰), which is certified by the International Atomic Energy Agency (Vienna, Austria). The precision for bulk-element contents was better than ±0.1 wt%. The precisions for each bulk isotopic value were better than ±0.1 ‰ and ± 0.3 ‰, respectively.

2.3. Extraction, separation, and purification

A 10-g aliquot of freeze-dried sediment was extracted using an ASE 200 extractor (Dionex, CA, USA) with a solvent mixture of dichloromethane (DCM) and methanol (MeOH) at a 9:1 ratio (v:v) and high temperature and pressure (100 °C and 1500 psi). Internal standards of 5α-androstane and 2-fluorobiphenyl were added for quantification of *n*-alkanes and PAHs, respectively. Lipid analytical procedures were formed as described by Lee et al. (2018a, b). Briefly, the total lipid extract (TLE) was passed through an anhydrous Na_2SO_4 column. The TLE was separated into aliphatic and aromatic hydrocarbon fractions according to the polarity of the compounds in an SiO_2 column (activated for 2 h at 150 °C). The aliphatic fraction was eluted using hexane (100 %), and the aromatic fraction was eluted using hexane and DCM at a ratio of 8:2 (v:v). The eluent was concentrated using a gentle stream of nitrogen and transferred into a gas chromatography (GC) vial. For further purification in stable-isotope analysis, the *n*-alkanes fraction was passed through a Ag^{2+}-impregnated silica gel with hexane. The PAHs were purified through thin-layer chromatography (TLC) to remove interfering compounds. A 60 Å TLC silica-gel plate (Merck, Darmstadt, Germany) cut to a length of 10 cm and a width of 4 cm was pre-cleaned using DCM (1:1, *v*/v), and then activated at 120 °C for 1 h. After the TLC plate cooled, a 1 cm mark was made with graphite to ensure the sample would not directly contact the carrier-solvent mixture. The concentrated PAH fraction was then loaded onto a TLC plate that had been eluted with a solvent mixture of cyclohexane:toluene at a ratio of 3:2 (v:v). A thin band of the TLC plate containing PAHs ($R_f \sim 0.81$) was confirmed under short-wavelength (254 nm) ultraviolet light. The TLC plate with PAHs was cut out and was extracted by sonication. The purified compounds were subsequently concentrated to 40 μL using N_2 gas to ensure a sufficient amount of the compound for analysis.

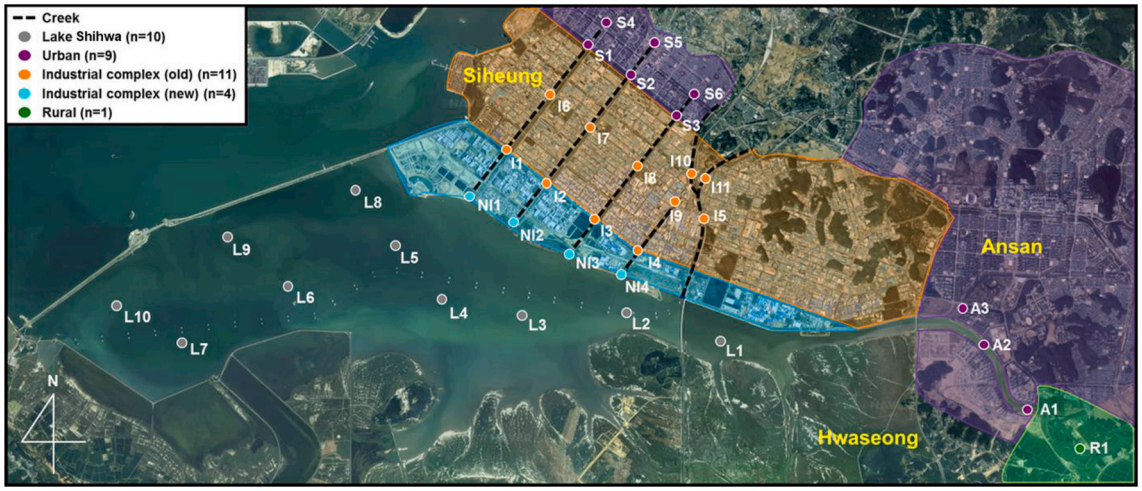

Fig. 1. Information on sampling sites with categorized land-use types (rural, urban, industrial complexes) near Lake Shihwa.

2.4. Gas chromatography and gas chromatography–mass spectrometry

All aliphatic and aromatic hydrocarbons fractions were analyzed using a 7890B GC apparatus (Agilent, USA) coupled to a 5977B mass spectrometer (MS; Agilent, CA, USA) operating at 70 eV. A fused-silica capillary column (HP-5MS; 30 m × 0.25 mm internal diameter [i.d.]; film thickness of 0.25 μm; Agilent, CA, USA) was used with helium as a carrier gas. The aliphatic hydrocarbons were injected under a constant flow (1 mL/min) at an initial oven temperature of 70 °C. The oven temperature was programmed to increase from 70 °C to 130 °C at 20 °C/min and then at 4 °C to a final temperature of 320 °C with a final hold time of 25 min. The aromatic hydrocarbons were injected under same helium flow. The initial oven temperature of 60 °C was held for 2 min, then raised to 200 °C at 10 °C/min, increased to 240 °C at 2 °C/min and held for 10 min, and then to a final temperature of 300 °C, with a final hold time of 10 min. The *n*-alkanes were identified from ion fragments, and their concentrations were determined by comparing peak areas with those of 5α-androstane, using a GC flame ionization detector with a fused-silica capillary column (DB-5, 60 m × 0.25 mm i.d.; film thickness of 0.25 μm; Agilent, CA, USA). PAHs were identified from ion fragments, and their concentrations were obtained in selective ion monitoring mode.

2.5. Gas chromatography-combustion isotope-ratio mass spectrometry

The $\delta^{13}C$ values of each compound were determined using an isotope-ratio mass spectrometer connected to a gas chromatograph via a combustion interface (a glass tube packed with copper oxide operated at 850 °C). The samples were subjected to the same temperature conditions and capillary column described for the GC and GC–MS analyses. Isotopic values were expressed as $\delta^{13}C$ values per mil relative to Vienna Peedee Belemnite. The analytical errors were <0.4 ‰ for all compounds.

2.6. Source-recognition ratio

Chemical indices were calculated using the concentrations of *n*-alkanes and PAHs. For *n*-alkanes, the terrestrial-to-aquatic ratio (TAR; odd long-chain *n*-alkanes/even short-chain *n*-alkanes; >5 = terrestrial sources, <1 = aquatic sources, Bourbonniere and Meyers, 1996), average chain length (ACL; ~30 = higher plants, ~29 = marine origin, ~28 = petrogenic sources, Cranwell et al., 1987; Poynter and Eglinton, 1991), percent of aquatic macrophyte input ($P_{mar\text{-}aq}$; 0.01–0.25 = terrestrial input, 0.4–0.6 = emergent aquatic plant, >0.6 = macrophyte input, Ficken et al., 2000; Mead et al., 2005), carbon preference index (CPI; >5 = higher terrestrial plants, ~1 = petrogenic sources, Bray and Evans, 1961), natural *n*-alkanes ratio (NAR; ~0 = petroleum sources, >1 higher terrestrial or aquatic plant, Mille et al., 2007), and pristane/phytane value (Pr/Ph; <1 = petroleum input, Zaghden et al., 2017):

$$TAR = \frac{[C27 + C29 + C31]}{[C15 + C17 + C19]} \quad (1)$$

$$ACL = \frac{[25 \times C25 + 27 \times C27 + 29 \times C29 + 31 \times C31 + 33 \times C33]}{[C25 + C27 + C29 + C31 + C33]} \quad (2)$$

$$P_{mar-aq} = \frac{[C23 + C25]}{[C23 + C25 + C29 + C31]} \quad (3)$$

$$CPI = \frac{1}{2} \times \left[\left(\frac{[C25 + C27 + C29 + C31 + C33]}{[C24 + C26 + C28 + C30 + C32]} \right) + \left(\frac{[C25 + C27 + C29 + C31 + C33]}{[C26 + C28 + C30 + C32 + C34]} \right) \right] \quad (4)$$

$$NAR = \frac{[\sum C19\text{–}C32] - [2 \times (\sum \text{even } C20\text{–}C32)]}{[\sum C19\text{–}C32]} \quad (5)$$

$$Pr/Ph = \frac{\text{Pristane}}{\text{Phytane}} \quad (6)$$

where C_n is the concentration of the *n*-alkane containing n carbon atoms.

2.7. Statistical analysis

The fractional abundances of *n*-alkanes ($n\text{-}C_{16} - n\text{-}C_{35}$, pristane, and phytane) and PAHs (Phe, Ant, Pyr, Fl, BaA, Chry, BbF, BaP, IcdP, DahA, and BghiP) were obtained by normalizing each concentration to a summed concentration. Principal component analysis (PCA) was performed on the fractional abundance data of each parameter to provide a general view of the variability of the distribution of each parameter

using R (version 4.0) and FactomineR (version 2.4).

2.8. Bayesian mixing model

To estimate the proportional contributions among various OM sources, such as terrestrial C3 plants, petroleum, and combustion, we used $\delta^{13}C$ values of *n*-alkanes and PAHs at our study sites. For representative end members, the isotopic compositions $\delta^{13}C_{n\text{-alkanes}}$ and $\delta^{13}C_{PAHs}$ derived from each source were − 37.0 ± 1.6 ‰ and − 28.5 ± 1.5 ‰ for terrestrial C_3 plants, −28.4 ± 1.6 ‰ and − 26.9 ± 0.2 ‰ for petroleum, and − 31.6 ± 0.5 ‰ and − 23.3 ± 2.3 ‰ for combustion, respectively (Abrajano Jr. et al., 2003; Cooper et al., 2015; Gao et al., 2018; McRae et al., 1999; Okuda et al., 2003; O'malley et al., 1994; O'malley et al., 1997; Peng et al., 2006; Wilhelms et al., 1994). At least, the application of these isotopic signatures may be suitable for estimating source contributions by comparing indigenous values reported in the surrounding areas of Lake Shihwa (Kim et al., 2017; Kim et al., 2018). Based on these literatures, $\delta^{13}C$ values of specific compounds (*n*-alkanes: C_{27}, C_{29}, C_{31}; PAHs: Fl, Pyr, BaA, Chry, IcdP, BghiP) were used to estimate the source contributions of each OM sample. All analyses were performed using R (version 4.0) and the MixSIAR package (version 3.1).

3. Results and discussion

3.1. Spatial characteristics of bulk elements

The TOC contents of the sediments were 3.9 ± 3.2 % for urban areas, 6.3 ± 6.8 % for old industrial complexes, 0.6 ± 0.3 % for new industrial complexes, 3.9 % for rural areas, and 0.7 ± 0.3 % for Lake Shihwa. The TN contents were 0.1 ± 0.1 % for urban areas, 2.3 ± 6.1 % for old industrial areas, < 0.1 % for new industrial areas, 0.2 ± 0.1 % for rural areas, and < 0.1 % for Lake Shihwa (Fig. 2). The $\delta^{13}C_{TOC}$ values were − 25.6 ± 1.1 ‰ for urban areas, −25.9 ± 1.7 ‰ for old industrial complexes, −23.5 ± 0.7 ‰ for new industrial complexes, −29.0 ‰ for rural areas, and − 22.1 ± 1.0 ‰ for Lake Shihwa. The $\delta^{15}N_{TN}$ values were 3.5 ± 2.7 ‰ for urban areas, 1.7 ± 1.9 ‰ for old industrial complexes, 5.0 ± 1.2 ‰ for new industrial complexes, 8.6 ± 0.0 ‰ for rural areas, and 6.7 ± 0.8 ‰ for Lake Shihwa (Fig. 2). The TOC contents at urban areas (average of A1, A2, A3, S1, S2, S3, S4, S5, and S6) and old industrial complexes (average of I1, I2, I3, I4, I5, I6, I7, I8, I9, I10, and I11) were much higher than those of other land-use types (< 0.9 wt%; Fig. 2 and Table 1). With respect to the significant increase in TOC content (> 24 wt%) at I4, these increased patterns may be involved in the large discharge of sewage sludge derived from industrial activities within the Lake Shihwa watershed (Kim et al., 2018; Lee et al., 2018a; Moon et al., 2012). Regarding the spatial abundance of toxic compounds (e.g., organophosphate flame retardants, perfluorinated alky compounds; and polybrominated diphenyl ethers) were higher near urban boundaries (Lee et al., 2017a; Lee et al., 2018b; Rostkowski et al., 2006), and the predominant TOC contents at I4 may be closely related to increases in anthropogenic activities such as textile, automobile, and electrical appliance manufacturing and petrochemical industries (Lee et al., 2017b; Moon et al., 2012; Rostkowski et al., 2006). In addition, TN contents were largely increased (~21 wt%) at old industrial complexes (I1, shown in Fig. 2). For lake and river systems, including various land-use types, TN sources may originate from nitrogen-fixing organisms, atmospheric deposition, fossil-fuel combustion, fertilizer production,

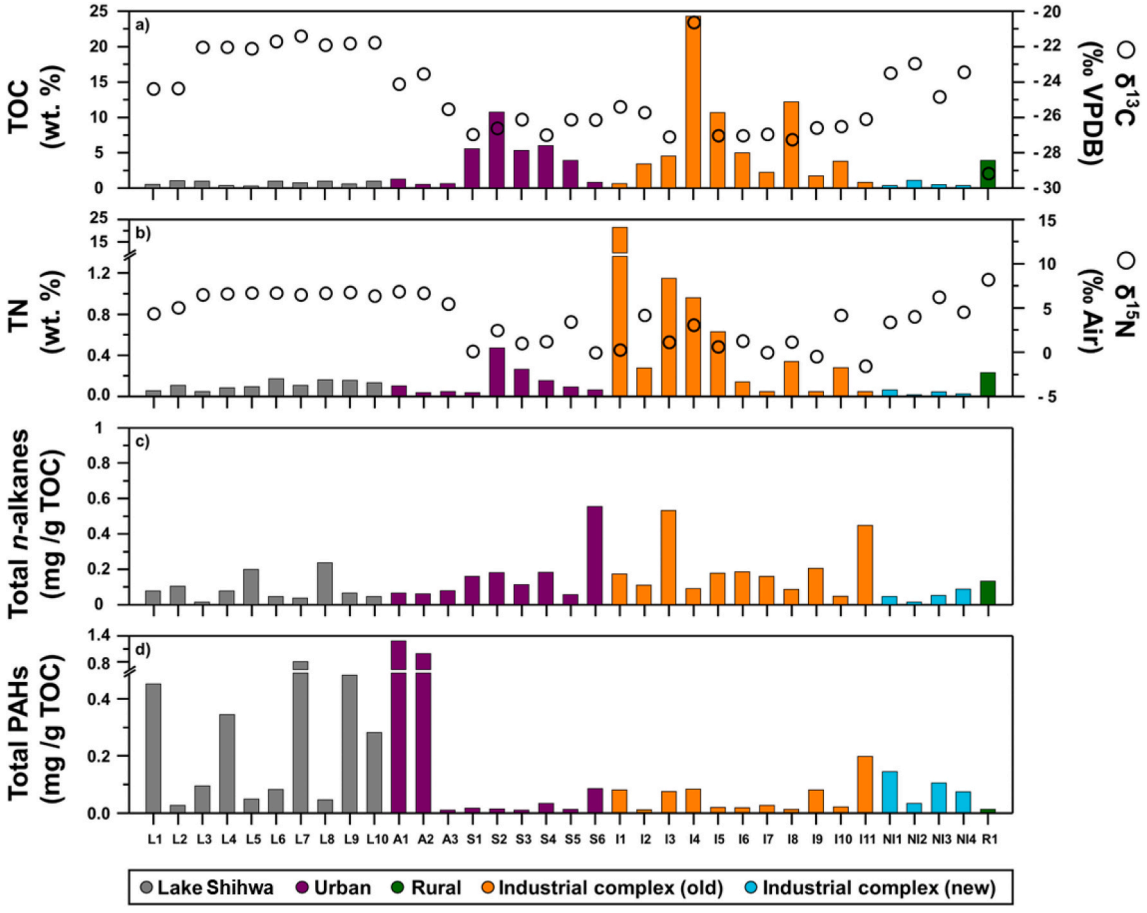

Fig. 2. Spatial distribution of (a) TOC contents and their isotopic compositions, (b) TN contents and their isotopic compositions, abundance of (c) total *n*-alkanes and (d) total PAHs.

Table 1
The bulk contents and isotopic compositions of sedimentary carbon and nitrogen.

Land use type	Site	Bulk element			
		TOC		TN	
		wt%	‰ VPDB	wt%	‰ air
Lake Shihwa	L1	0.5	−24.2	0.1	4.8
	L2	1.0	−24.1	0.1	5.5
	L3	1.0	−21.8	0.0	6.9
	L4	0.4	−21.8	0.1	7.0
	L5	0.3	−21.9	0.1	7.1
	L6	1.0	−21.5	0.2	7.1
	L7	0.7	−21.2	0.1	6.9
	L8	1.0	−21.7	0.2	7.1
	L9	0.6	−21.6	0.2	7.2
	L10	1.0	−21.6	0.1	6.8
Urban	A1	1.3	−23.9	0.1	7.3
	A2	0.5	−23.3	0.0	7.1
	A3	0.7	−25.3	0.0	5.9
	S1	5.5	−26.7	0.0	0.5
	S2	10.7	−26.4	0.5	2.9
	S3	5.3	−25.9	0.3	1.4
	S4	6.0	−26.8	0.2	1.6
	S5	3.9	−25.9	0.1	3.9
	S6	0.8	−25.9	0.1	0.4
Old industrial complex	I1	0.7	−25.2	21.5	0.7
	I2	3.4	−25.5	0.3	4.6
	I3	4.5	−26.9	1.1	1.6
	I4	24.8	−20.9	1.0	3.5
	I5	10.6	−26.8	0.6	1.1
	I6	5.0	−26.8	0.1	1.7
	I7	2.2	−26.7	0.0	0.4
	I8	12.2	−27.0	0.3	1.6
	I9	1.7	−26.4	0.0	0.0
	I10	3.8	−26.3	0.3	4.6
	I11	0.8	−25.9	0.0	−1.1
New industrial complex	NI1	0.4	−23.3	0.1	3.8
	NI2	1.1	−22.7	0.0	4.5
	NI3	0.5	−24.6	0.0	6.7
	NI4	0.3	−23.2	0.0	5.0
Rural	R1	3.9	−28.9	0.2	8.6

and wastewater (Elliott and Brush, 2006; Howarth, 2008; Ohkouchi and Takano, 2013). With respect to the increased nitrogen loading derived from the effluent of wastewater treatment plants (Lee et al., 2017b) flowing into the Lake Shihwa watershed, the high TN contents at I1 may be due to the substantial export of wastewater within industrial complex. Meanwhile, spatial variations between TOC and TN showed negligible correlations along sampling sites ($R^2 = 0.1, p > 0.10$). Various forms of OM were heterogeneously exported by different land-use types within Lake Shihwa (Lee et al., 2017b; Moon et al., 2012; Oh et al., 2010), and these patterns may reflect the mix of contributions from natural and anthropogenic OM.

The isotopic signature of OM has been often used to distinguish autochthonous and allochthonous origins, because different isotopic fractionation occurs between reactant and product (Canuel and Hardison, 2016; Thornton and McManus, 1994). In this study, $\delta^{13}C_{TOC}$ values were more enriched (−22.1 ± 1.0 ‰) in lake sediment, compared to those of land-use types (urban: −25.6 ± 1.1 ‰; old industrial complexes: −25.9 ± 1.7 ‰; new industrial complexes: −23.5 ± 0.7 ‰; and rural: −29 ‰; Table 1 and Fig. 2). Typically, $\delta^{13}C$ values of various OMs showed discriminative isotopic ranges (−10 ‰ to −30 ‰ for terrestrial C_3 and C_4 plants; −24 ‰ to −18 ‰ for phytoplankton; −62 ‰ to −6 ‰ for bacteria; and − 27 ‰ to −25 ‰ for anthropogenic sources organic fertilizer and sludge) (Derrien et al., 2018; Fry and Sherr, 1989; Parat et al., 2007; Vuorio et al., 2006). The most depleted $\delta^{13}C$ values at rural areas (R1) may be related to the specific metabolic pathway of terrestrial C_3 plants (Chikaraishi et al., 2004; Smith and Epstein, 1971), indicating their predominance within a rural boundary. However, $\delta^{13}C_{TOC}$ values at new industrial complexes showed significantly enriched patterns ($p <$ 0.05) compared with those of urban areas and old industrial complexes (Fig. 2). With respect to the isotopic signatures (−16 ‰ to −24 ‰) derived from carbon fixation of phytoplankton (Fry and Sherr, 1989; Gu et al., 2006; Xu et al., 2019), ^{13}C-enriched patterns at these sites can provide the evidence of predominant algal communities that accumulate in sediment. Actually, considering anthropogenic derived-nitrates near industrial complexes can be predominantly transported into water column of Lake Shihwa (Kim et al., 2024), variation in elemental ratios (nitrogen and phosphate) may influence in situ biosynthesis of algal communities (Inomura et al., 2022). As another possibility involved in the presence of C_4 plants, we confirmed the absence of terrestrial C_4 plant in our study site (Lee et al., 2017b; Kim et al., 2022). Based on these literatures, we consider that these C_4 plant sources as the potential OM end-members may be excluded for tracing OM source in Lake Shihwa. Meanwhile, the overlapping $\delta^{13}C_{TOC}$ values (−25.9 ± 1.7 ‰) from urban areas (A1, A2, A3, S1, S2, S3, S4, S5, S6) and old industrial complex (I1, I2, I3, I4, I5, I6, I7, I8, I9, I10, I11) may reflect the mixed signatures of various source of OM (e.g., terrestrial C_3 plants, phytoplankton, sludge, organic fertilizer, and bacteria). Among them, the more ^{13}C-enriched signatures at I4 showed mixed signatures for anthropogenic and natural sources (Bosch et al., 2015; Derrien et al., 2018; Fry and Sherr, 1989; Gleason and Kyser, 1984; Vuorio et al., 2006; Maksymowska et al., 2000; Spies et al., 1989). Together with the export of point sources (e.g., municipal sewage treatment plants), these patterns appear to provide evidence for a mixed contribution transported via unintentional non-point sources (e.g., atmospheric deposition and surface runoff).

The $\delta^{15}N_{TN}$ values were more enriched in rural area R1 (8.6 ‰) compared with other land-use types (urban areas: 3.5 ± 2.6 ‰; old industrial complexes: 1.7 ± 1.8 ‰; and new industrial complexes: 5.0 ± 1.1 ‰; Table 1 and Fig. 2). For lake and river systems, $\delta^{15}N_{TN}$ values have broad isotopic variations (e.g., forest leaf: −1.4 ± 1.1 ‰; C3 plant: 7.4 ± 1.9 ‰; C4 plant: 10.7 ± 0.2 ‰; organic fertilizer: 9.2 ± 3.4 ‰; and sewage: 3.3 ± 2.7 ‰) (Debruyn and Rasmussen, 2002; Derrien et al., 2018; Elliott and Brush, 2006; Dover et al., 1992). Among them, according to the frequent use of organic fertilizers at the agriculture boundary (Diebel et al., 2009), ^{15}N-enriched isotopic compositions at R1 may reflect the export of some organic fertilizers (e.g., oilcake and manure), which was characterized with ammonia volatilization and denitrification (Derrien et al., 2018; Vitòria et al., 2004; Bottchew et al., 1990; Diebel et al., 2009). Meanwhile, more ^{15}N-depleted isotopic signatures at some sites (S1, S2, S3, S4, I1, I2, I7, I9) may be indicative of increased export of wastewater derived from urban areas and old industrial complexes (Elliott and Brush, 2006; Lee et al., 2014). These patterns are supported by previous N-isotopic signatures (−3.4 ‰ to 7.7 ‰) derived from anthropogenic sources via outfall pipes at Shihwa industrial complexes (Lee et al., 2017b; Hong et al., 2019). Based on different signatures of $\delta^{15}N_{TN}$ values associated with various land-use types, the $\delta^{15}N_{TN}$ values at Lake Shihwa (4.8 ‰ to 7.2 ‰) appear to be heterogeneously influenced by a mix of exports of natural sources (e.g., terrestrial C_3 plant, algae, and bacteria) and anthropogenic sources (e.g., fertilizer and sewage). To effectively constrain the intrinsic characterization of mixed OM sources within Lake Shihwa, we further investigated spatial variations of molecular biomarkers that can provide source specificity and conservative behavior of mixed OM.

3.2. Spatial variations of n-alkanes and PAHs

Short-chain and long-chain *n*-alkanes (*n*-C_{16} to *n*-C_{35}), as well as other saturated alkanes and pristane and phytane compounds with an unresolved complex mixture were found at all sites (supplementary information Fig. S1). Corresponding to spatial variations of TOC abundances measured at each sampling site, the abundance of lipid molecules was commonly normalized by using TOC abundances. The TOC-normalized concentrations of alkanes were 0.2 ± 0.2 mg/g for urban areas and 0.2 ± 0.2 mg/g for old industrial complexes, indicating higher

concentrations compared with those found in other land-use types, such as new industrial complexes (< 0.1 mg/g TOC), rural areas (0.1 ± 0.0 mg/g), and Lake Shihwa (0.1 ± 0.1 mg/g) (Fig. 2, and Table 2). The total PAH concentrations (for Phe, Ant, Fl, Pyr, BaA, Chry, BbF, BaP, IcdP, DahA, and BghiP) were 0.3 ± 0.5 mg/g TOC for urban areas, 0.1 ± 0.1 mg/g for old industrial complexes, < 0.1 mg/g for new industrial complexes, < 0.1 mg/g for rural areas, and 0.3 ± 0.2 mg/g for Lake Shihwa (Fig. 2 and Table 3). Based on spatial variations of both compounds within different land-use types, including lake sediments, we performed a PCA using the relative abundance of these compounds normalized by TOC content (Fig. 3). For *n*-alkanes, PC1 and PC2 accounted for 27.5 % and 20.0 % of total variance, respectively (cumulative 47.6 % of variance). The odd-numbered long-chain *n*-alkanes (*n*-C_{27}, *n*-C_{29}, *n*-C_{31}) are closely related to each other, representing negative correlations with PC1. In contrast, the short/even-numbered *n*-alkanes, pristane, and phytane variables were positively loaded to PC1. PC2 showed a positive correlation with those in the Lake Shihwa while representing a negative correlation with those in urban areas. Meanwhile, as shown in Fig. 3, PC1 and PC2 accounted for 52.0 % and 17.5 % of variables, respectively. In PC1, the highly conjugated aromatic hydrocarbons (IcdP, BghiP) at Lake Shihwa were opposite to those of low molecular-weight aromatic hydrocarbons (Phe, Ant, Pyr, Fl). PC2 showed a weak positive correlation with the sediment from Lake Shihwa while representing a slightly negative correlation with sediment from urban areas.

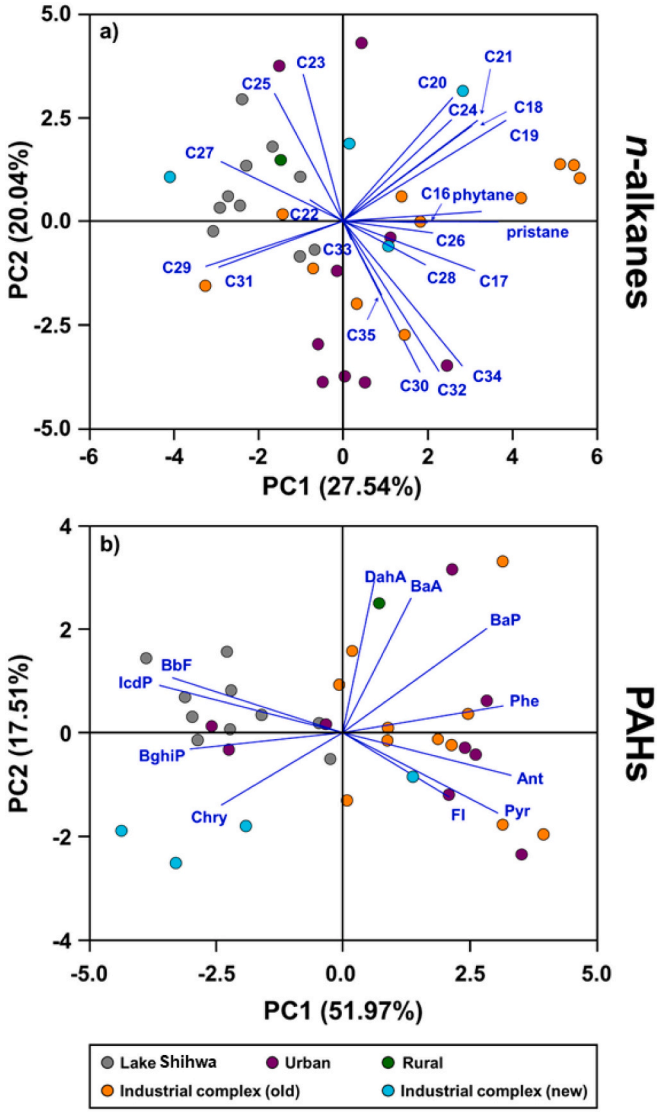

Fig. 3. Principal component analysis of fractional abundance of (a) *n*-alkanes and (b) PAHs.

With respect to the predominant abundance of long-chain alkanes (i.e., *n*-C_{27}, *n*-C_{29}, *n*-C_{31}) at Lake Shihwa and rural areas, these compounds may be typically originated from terrestrial higher plants (Meyers, 2003). In contrast, odd short-chain alkanes (i.e., *n*-C_{15}, *n*-C_{17}, *n*-C_{19}) and even short-chain alkanes (i.e., *n*-C_{16}, *n*-C_{18}, *n*-C_{20}) were predominant at old industrial complexes and urban areas, reflecting natural (e.g., algae, bacteria and macrophyte) and anthropogenic (e.g., coal and petroleum) origins, respectively (Gelpi et al., 1970; Meyers, 2003; Mille et al., 2007; Rojo, 2009; Wang et al., 2010). In this regard, aliphatic hydrocarbons are indicative of source origins and diagenesis/catagenesis processes by environmental changes, as patterns of the odd- to even-chain numbers in aliphatic hydrocarbons may be changed by selective degradations and/or cleavage of the C—C bond (Tareq et al., 2005). At least, the patterns of this aliphatic compound investigated at our study may be attenuated under higher biodegradability (Kim et al., 2018). To resolve these aspects, we considered the integration of aromatic hydrocarbons for effectively determining anthropogenic sources such as petroleum and combustion origins. With respect to the increased abundance of LMW PAHs (2 to 3 aromatic rings; Phe and Ant) at urban areas and old industrial complexes (Table 3), such compounds derived from petrogenic sources may be associated with the use of plastic waste and crankcase oil (Conesa et al., 2021; Lee et al., 2018b). According to PCA results which are potentially related to the substantial transport of petroleum sources, the origin of these LMW PAHs may be influenced by substantial transport of petroleum sources under extensive industrial activities surrounding Lake Shihwa. By contrast, the predominant abundance of higher-molecular-weight (HMW) PAHs (4 to 6 aromatic rings; BaA, Chry, BbF, BaP, DahA, BghiP, and IcdP) at old industrial complexes and urban areas may be related to the source contribution (e.g., petroleum and combustion) derived from anthropogenic activities near Lake Shihwa (Abdel-Shafy and Mansour, 2016). The abundance of these PAHs increased continuously at industrial complex boundaries, which could be related to the fossil fuels used in industrial activities over the last decades (Dai et al., 2022; Kwon and Choi, 2014). In addition, with respect to the increase of HMW PAHs in urban boundaries, these compounds may be introduced via atmospheric depositions such as soil road dust, vehicular exhausts, inland heating combustion, and incineration (Bian et al., 2016; Kim and Chae, 2016). These properties might reflect the continuous contamination of anthropogenic sources near Lake Shihwa.

Based on spatially discriminative patterns of natural and anthropogenically derived compounds, we compared spatial variations of specific *n*-alkane indices (e.g., TAR, ACL, $P_{mar\text{-}aq}$, CPI, NAR, Pr/Ph ratio) along different land-use types (Fig. 4). First, TAR values ranged from 2.5 to 30.0, showing relatively higher patterns at Lake Shihwa, compared with those of old industrial complexes (I2, I3, I4, I5, I7, I9, I11). The increased TAR values (> 5) may reflect the predominant input of terrestrial plants within the Lake Shihwa (Ortiz et al., 2013; Silliman et al., 1996). However, other indices (ACL and $P_{mar\text{-}aq}$) showed insignificant differences ($p > 0.11$ and $p > 0.26$, respectively) among land-use types (Fig. 4), reflecting ubiquitous distribution of epicuticular leaf wax into Lake Shihwa (Ficken et al., 2000; Mead et al., 2005; Sikes et al., 2009; Kim et al., 2018). Based on these indices, terrestrial plant sources within each land-use type may be heterogeneously transported into Lake Shihwa. Meanwhile, CPI, NAR and Pr/Ph values are often used to estimate specific OM origins and their diagenetic processes (Peters et al., 2007; Volkman et al., 1992). For CPI values, each value (1.1 to 6.8 for CPI) showed overlapping patterns between most sites (Fig. 4). Among them, CPI values were much closer to 1 at urban areas (S3, S4, S6) and old and new industrial complexes (I4, I7, I9, I11, NI2) compared with those of other land-use types. Together with CPI values, NAR values, which can roughly estimate the proportions of natural and petroleum (Mille et al., 2007; Sojinu et al., 2012), showed a spatially overlapped

Table 2
The concentrations of *n*-alkanes within land-use boundaries.

Land use type	Site	Aliphatic hydrocarbon (μg/gTOC)																					
		C16	C17	Pr	C18	Ph	C19	C20	C21	C22	C23	C24	C25	C26	C27	C28	C29	C30	C31	C32	C33	C34	C35
Lake Sihwa	L1	0.2	0.4	0.1	1.7	0.2	1.4	1.8	2.4	2.6	3.3	2.7	4.6	2.5	8.0	3.5	13.4	2.8	11.6	2.9	6.3	1.8	2.1
	L2	0.7	1.1	0.9	1.9	1.9	1.7	1.8	1.8	2.1	2.8	2.0	5.6	3.5	8.8	4.8	15.5	4.4	22.6	4.3	10.1	2.9	2.3
	L3	0.3	0.1	0.0	0.1	0.0	0.2	0.4	0.4	0.5	0.7	0.4	1.0	0.5	1.5	0.6	2.4	0.4	2.3	0.4	1.0	0.2	0.3
	L4	0.3	0.8	0.2	0.7	0.2	0.9	1.3	1.7	1.8	3.1	2.2	4.6	1.9	7.6	3.1	14.7	2.3	14.9	2.6	7.0	1.4	1.8
	L5	0.8	1.4	1.5	2.4	2.0	2.7	2.7	3.7	4.9	6.0	6.4	11.0	6.0	17.2	7.3	31.1	7.6	37.2	8.5	24.2	7.2	6.5
	L6	0.1	0.3	0.1	0.4	0.1	0.5	0.4	0.7	0.9	1.7	1.1	2.6	1.4	4.9	1.9	9.3	1.6	9.0	1.3	4.1	0.6	1.2
	L7	0.1	0.2	0.0	0.3	0.0	0.4	0.9	1.0	1.4	2.3	1.8	3.1	1.4	4.1	1.5	6.4	1.0	5.5	0.8	2.2	0.3	0.6
	L8	0.4	0.7	0.6	1.4	0.5	1.2	1.6	1.9	17.2	2.4	2.6	3.5	2.4	6.2	2.8	10.1	2.7	11.7	2.3	6.2	1.2	1.5
	L9	0.1	0.4	0.2	1.0	0.1	1.1	1.3	1.5	8.8	2.5	1.6	3.9	2.0	6.3	2.4	11.4	1.7	10.7	1.5	4.6	0.7	1.3
	L10	0.1	0.2	0.2	0.5	0.2	0.6	0.5	1.0	1.4	1.7	1.0	2.7	1.5	4.9	1.6	8.5	1.4	8.8	1.1	3.7	0.5	1.2
Urban	A1	0.2	0.6	0.1	2.5	0.2	1.3	2.8	1.4	2.0	3.9	3.1	5.6	1.8	6.2	1.9	11.1	1.7	11.0	1.5	4.6	0.8	1.0
	A2	0.3	0.4	0.1	2.6	0.2	1.8	4.5	1.4	3.5	3.6	2.8	4.5	1.8	5.7	2.5	7.6	1.7	7.3	1.8	4.3	1.0	1.2
	A3	0.4	1.4	0.2	2.6	0.4	1.6	2.8	2.3	3.6	2.5	2.8	3.4	2.6	4.6	2.9	9.4	4.0	14.2	4.4	7.6	3.5	2.2
	S1	0.5	1.8	1.6	1.6	2.3	1.3	2.0	1.9	2.9	3.8	3.7	7.0	4.9	12.0	7.3	29.8	10.2	30.3	11.1	12.7	8.0	3.9
	S2	1.5	7.9	1.2	2.2	2.1	2.0	2.3	2.4	2.7	3.0	3.3	6.2	4.2	11.5	6.8	28.0	11.4	33.4	14.3	17.2	10.3	5.3
	S3	0.7	3.6	0.5	1.5	1.0	1.0	1.5	1.2	2.1	1.9	2.5	4.1	3.5	7.3	5.0	20.2	7.7	20.1	9.1	9.0	6.2	2.7
	S4	0.5	2.2	0.3	2.4	0.7	1.5	2.9	1.7	3.5	3.3	4.2	6.2	6.4	11.7	7.9	34.5	13.3	33.8	14.2	15.4	11.1	4.8
	S5	0.3	0.7	0.3	1.0	0.6	0.8	1.3	1.0	1.4	1.8	1.8	2.7	2.1	4.8	2.5	10.0	3.0	8.8	3.3	3.7	2.6	1.2
	S6	4.1	9.3	2.6	13.0	4.4	8.6	15.5	8.1	17.1	10.8	19.3	17.6	24.8	30.3	33.1	72.8	46.9	77.0	52.4	37.0	37.0	10.6
Old industrial complex	I1	1.1	1.5	0.7	4.2	1.0	2.2	4.0	3.6	5.2	4.9	6.2	8.0	4.6	12.1	5.5	27.2	5.8	45.3	6.5	15.7	4.9	2.3
	I2	1.3	8.1	2.7	3.0	10.9	3.8	2.9	6.5	3.0	1.9	3.2	3.9	3.0	4.7	3.5	11.3	2.9	13.8	2.8	11.4	2.4	2.0
	I3	6.2	20.9	5.2	7.5	12.0	9.1	10.3	22.3	24.5	15.1	27.1	26.3	12.8	38.5	17.0	63.4	17.2	82.1	22.7	62.1	17.1	10.9
	I4	1.8	3.5	1.3	3.0	2.5	2.6	3.4	2.5	5.2	2.0	5.4	3.0	3.7	4.8	3.5	9.0	3.8	9.8	3.8	10.1	3.9	1.8
	I5	2.1	7.9	3.7	5.0	4.5	5.1	4.0	5.1	4.3	5.0	4.5	8.8	4.4	14.4	6.3	32.9	8.4	23.9	8.4	10.1	5.9	3.5
	I6	0.9	3.4	0.7	2.3	1.4	2.0	2.9	2.8	3.3	5.2	6.4	12.0	8.2	15.9	8.8	36.2	11.4	30.0	9.3	10.9	7.4	3.0
	I7	1.0	7.3	0.8	2.9	1.3	2.3	3.4	2.8	4.4	3.6	5.0	6.3	5.7	10.2	7.3	22.6	9.3	25.1	11.8	11.9	9.6	4.4
	I8	1.5	1.6	0.6	1.4	1.0	0.9	1.3	2.4	1.7	1.4	2.3	3.5	2.3	7.0	3.5	13.1	4.2	17.0	5.2	6.0	4.3	2.2
	I9	1.8	5.7	3.8	7.6	7.6	8.9	9.4	9.0	8.3	7.5	9.0	10.3	7.4	12.4	10.8	13.2	10.9	19.0	15.0	10.5	10.6	4.8
	I10	0.3	0.6	0.2	0.6	0.2	0.5	0.6	0.6	0.6	1.0	0.5	1.6	0.8	3.5	1.0	9.3	1.7	14.4	1.7	5.1	1.2	0.8
	I11	3.3	8.3	5.4	15.3	10.9	16.2	25.1	23.0	26.5	20.3	22.2	22.2	20.1	22.9	20.4	31.3	27.6	37.5	32.1	22.7	24.9	8.7
New industrial complex	NI1	0.3	0.4	0.1	1.1	0.4	1.0	1.5	1.4	1.8	1.8	1.7	2.7	1.7	3.9	1.7	5.7	1.6	7.0	1.4	4.5	0.9	0.9
	NI2	0.1	0.3	0.1	0.2	0.1	0.2	0.4	0.3	0.6	0.5	0.7	0.8	0.6	1.1	0.7	1.7	0.7	1.9	0.8	1.2	0.7	0.5
	NI3	0.1	0.6	0.1	0.4	0.1	0.5	1.3	0.8	1.2	2.1	1.2	3.4	1.1	4.6	1.1	9.6	1.2	16.3	1.5	4.2	0.3	0.6
	NI4	0.4	0.8	0.9	5.7	0.5	2.8	5.8	2.6	4.0	4.0	4.5	4.1	2.6	4.9	4.1	8.9	2.3	12.5	2.9	9.1	2.6	2.0
Rural	R1	1.1	2.6	0.4	3.1	1.3	2.3	2.2	3.4	3.0	10.7	3.4	7.3	3.1	10.5	5.9	26.4	6.1	24.6	5.0	6.7	2.0	1.6

Table 3
The concentrations of PAHs within land-use boundaries.

Land use type	Site	Aromatic hydrocarbon (μg/gTOC)										
		Phe	Ant	Fl	Pyr	BaA	Chry	BbF	BaP	IcdP	DahA	BghiP
Lake Sihwa	L1	2.7	0.5	52.8	38.4	24.6	51.1	75.2	20.8	82.0	16.6	86.8
	L2	1.0	0.3	3.9	3.8	1.4	2.3	3.1	1.4	3.2	0.8	4.3
	L3	0.3	0.1	6.7	6.5	5.5	11.0	17.7	3.9	19.6	4.5	19.4
	L4	1.1	0.6	35.2	28.5	18.8	37.1	59.0	16.8	64.7	13.6	68.5
	L5	1.1	0.3	7.3	6.9	3.0	4.5	6.1	2.9	6.4	1.9	8.9
	L6	0.8	0.2	11.0	7.1	4.9	8.4	13.7	4.4	14.4	3.1	14.1
	L7	1.5	0.3	89.2	69.7	60.0	99.5	130.3	45.7	139.3	31.9	133.4
	L8	1.1	0.4	6.3	4.7	2.6	4.3	6.9	2.5	7.5	1.6	8.0
	L9	4.4	1.4	58.3	39.8	26.0	62.0	71.0	22.2	84.7	16.6	95.6
	L10	4.4	1.0	37.9	24.2	15.9	34.2	40.3	15.1	48.4	9.4	50.3
Urban	A1	10.9	1.3	172.7	127.2	81.6	163.0	218.4	46.2	210.8	46.9	202.8
	A2	7.6	1.0	114.9	130.1	62.6	130.2	147.8	35.9	146.5	35.2	176.3
	A3	0.4	0.1	1.1	1.3	0.5	0.8	0.9	0.5	1.1	0.4	2.0
	S1	1.1	1.3	2.3	2.7	0.8	1.5	1.3	1.0	1.1	0.6	2.3
	S2	0.8	1.3	2.5	3.4	0.8	1.2	0.9	0.9	0.8	0.4	1.5
	S3	0.6	0.8	1.3	1.6	0.6	0.9	0.7	0.6	0.6	0.4	1.2
	S4	3.7	2.3	4.0	5.1	1.8	3.1	2.5	2.1	2.4	1.3	4.5
	S5	0.7	0.6	1.5	1.6	1.0	1.2	1.2	1.1	1.1	0.8	1.5
	S6	7.7	6.8	12.0	12.4	5.7	8.0	7.0	6.1	6.1	3.7	9.4
Old industrial complex	I1	2.8	0.4	10.3	9.8	6.0	8.1	8.8	7.1	11.1	2.8	13.7
	I2	0.4	0.1	1.2	1.7	0.5	1.0	0.9	0.7	1.2	0.7	2.3
	I3	3.7	0.7	9.6	13.4	3.4	7.9	5.9	4.2	6.8	2.9	16.9
	I4	4.9	0.9	11.7	13.0	5.1	8.6	7.7	6.5	8.5	2.4	13.6
	I5	2.0	1.1	2.4	3.1	1.2	1.7	1.5	1.4	1.4	0.8	2.7
	I6	1.1	1.0	2.6	3.1	1.0	1.6	1.5	1.3	1.3	0.7	2.5
	I7	3.0	1.4	2.7	3.7	2.0	2.0	2.3	2.3	2.1	1.7	3.0
	I8	0.8	0.7	1.3	1.7	0.7	1.3	1.2	0.9	1.0	0.5	2.5
	I9	2.7	5.0	24.8	11.2	4.3	7.1	5.5	5.2	4.7	2.8	6.7
	I10	2.5	1.1	2.5	2.9	1.1	2.2	1.9	1.3	1.6	0.8	2.6
	I11	17.6	16.6	38.7	42.2	12.2	17.8	12.1	10.6	9.2	5.6	15.1
New industrial complex	NI1	2.7	11.1	22.0	23.0	11.6	23.5	16.4	9.4	11.3	3.4	10.7
	NI2	0.3	0.2	3.2	3.9	1.3	5.9	4.1	1.1	4.5	0.9	7.4
	NI3	0.6	0.6	7.9	8.1	3.9	20.8	13.2	3.5	17.4	3.6	24.5
	NI4	1.8	0.3	8.0	11.0	3.0	8.9	8.2	3.0	10.0	2.2	16.6
Rural	R1	0.2	0.0	0.4	0.3	0.2	0.3	0.4	0.2	0.4	0.2	0.3

pattern (−0.7 to 0.6; shown in Fig. 4) within land-use types, including Lake Shihwa. These patterns may indicate a mix of contributions from natural and anthropogenic OM. In this regard, lower values (< 1) of Pr/Ph may support the existence of petroleum-derived OM at sedimentary environments (Zaghden et al., 2017), reflecting the increased maturity of OM transported from urban areas and older industrial complexes.

The source-recognition ratio of PAHs (*m/z* 178; Phe, Ant, m/z 202; m/z 228; BaA, Chry, m/z 276; IcdP, BghiP) is often used to provide specific evidence regarding anthropogenic sources, and petroleum and combustion origins in particular (Yunker et al., 2002). In this regard, specific PAH indices showed varied ranges (Ant/(Ant+Phe); 0.1–0.8, BaA/(BaA + Chry); 0.2–0.5, Fl/(Fl + Pyr); 0.4–0.7, IcdP/(IcdP+BghiP); 0.3–0.5) along land-use types near Lake Shihwa (Fig. 5). Generally, the increased ratios (> 0.1) of Ant/(Ant+Phe) have been represented for combustion origins (e.g., for carbonization of bituminous coal, coal tar or coal combustion [Oros and Simoneit, 2000; Wise et al., 1988]). A ratio > 0.4 for BaA/(BaA + Chry) is often considered evidence of combustion, while ratios <0.2 may reflect petroleum used in diesel oil, crude oil and lubricants (Grimmer et al., 1981; Grimmer et al., 1983; Wang et al., 1999). Meanwhile, other PAHs (Fl, Pyr, IcdP, BghiP) were the most definitive compounds, with large differences in thermodynamic stability. Ratios of 0.4–0.5 for Fl/(Fl + Pyr) reflect petroleum origins (e.g., liquid fossil fuel, vehicle and crude oil, and kerosene), while ratios >0.5 may be indicative of grass, wood, or coal combustion (Jenkins et al., 1996; Laflamme and Hites, 1978; Yunker et al., 2002). The IcdP/(IcdP+BghiP) value is <0.5 for petroleum (e.g., creosote and asphalt) and combustion (e.g., wood soot, combustion aerosols, and bush fire particles) (Jenkins et al., 1996; Wakeham et al., 1980). For this study, both values (Ant/[Ant+Phe] vs. Fl/[Fl + Pyr]) showed ambiguous patterns along land-use types, providing mixed signatures for petroleum combustion, and grass, wood, and coal combustion. For another dual-ratio pattern, BaA/(BaA + Chry) values showed significant differences ($p < 0.10$) between new industrial complexes (NI1, NI2, and NI3) and other land-use types, reflecting the predominant contribution of petroleum. In contrast, Fl/(Fl + Pyr) patterns at Lake Shihwa (L1−L10) were greater than those of other land-use types ($p < 0.05$), indicating increased deposition of combustion origins. These patterns may be closely related to the transportation and logistics industry (which use petrol engines) in the Shihwa/Banwol industrial complex, where the steel, petrochemical, machinery, and electronics industries are highly developed. Increased transportation and logistics activities in these regions may lead to a higher atmospheric influx of combustion-derived PAHs that are subsequently deposited into the water column of Lake Shihwa (Kim and Chae, 2016; Tobiszewski and Namieśnik, 2012). Finally, IcdP/(IcdP+BghiP) patterns at our study sites showed lower values near the industrial complexes (and I3 in particular), indicating a significant increase in petroleum combustion in vehicles (Tobiszewski and Namieśnik, 2012). Actually, together with the abundance of PAHs within air dust (e.g., PM 10 and PM 2.4) collected near Lake Shihwa (Baek et al., 2020; Kang et al., 2020; Kim et al., 2021), we may consider partial possibility of PAH contributions derived from air dust. Therefore, corresponding to the significant evidence of petroleum-derived OM at urban areas and industrial complexes, the mixed OM (e.g., from terrestrial plants, petroleum, and by-products of combustion) within Lake Shihwa appears to be heterogeneously deposited through atmospheric deposition, outfall pipe, and surface runoff. In such situations, the use of these lipid indices has limited potential for use in tracing intrinsic OM sources transported into a lake system as they may undergo secondary diagenetic process (e.g., decomposition and weathering) within sediment (Dvorská et al., 2011; Liu et al., 2021; Rojo, 2009). To

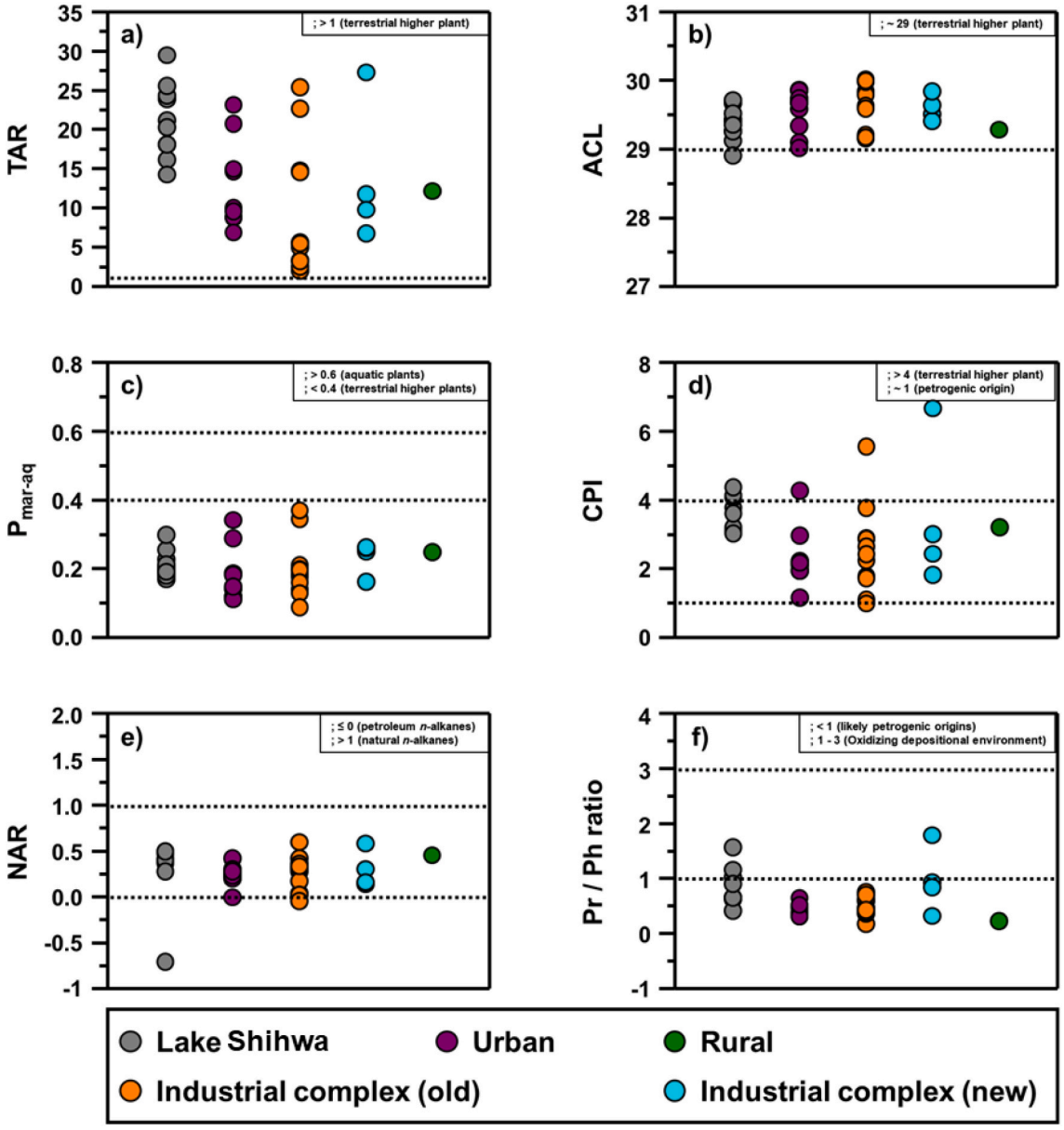

Fig. 4. Spatial variations of various *n*-alkane indices: (a) terrestrial/aquatic ration (TAR), (b) average chain length (ACL), (c) % of aquatic plants (Pmar-aq), (d) carbon preference index (CPI), (e) natural *n*-alkanes ratio (NAR), and (f) pristane/phytane (Pr/Ph).

fill the gap, CSIA approaches are consistently described as useful for estimating the relative proportion of mixed OM sources within complex natural systems (Fry, 2006; Parnell et al., 2013). With respect to reliable estimates of source apportionments, we used the isotopic data of *n*-alkanes and PAHs.

3.3. Isotopic signatures of n-alkanes and PAHs

CSIA approach has the potential to facilitate OM identification within natural sediments by exploiting differences in $\delta^{13}C$ values of lipid compounds (Marshall et al., 2007; Cooper et al., 2015). The $\delta^{13}C$ values of selected *n*-alkanes (*n*-C_{27}, *n*-C_{29}, *n*-C_{31}) ranged from −34.5 ‰ to −30.7 ‰ for urban areas, −39.8 ‰ to −34.0 ‰ for old industrial complexes, −35.7 ‰ to −27.5 ‰ for new industrial complexes, −35.2 ‰ to −34.3 ‰ for rural areas, and − 35.5 ‰ to −26.2 ‰ for Lake Shihwa, showing noticeably depleted values as carbon numbers increased. The $\delta^{13}C$ values of PAHs (Fl, Pyr, BaA, Chry, IcdP, BghiP) ranged from −27.4 ‰ to −24.3 ‰ for urban areas, −26.9 ‰ to −24.5 ‰ for old industrial complexes, −29.4 ‰ to −26.2 ‰ for new industrial complex, −30.3 ‰ to −26.4 ‰ for rural areas, and − 30.8 ‰ to −18.6 ‰ for Lake Shihwa (Fig. 6). Based on the predominance of odd long-chain *n*-alkanes (*n*-C_{27}, *n*-C_{29}, *n*-C_{31}) at sampling sites, $\delta^{13}C$ values of these compounds were significantly different in different types of land use (−32.9 ± 1.2 ‰ for urban areas, −35.7 ± 2.0 ‰ for old industrial complexes, −31.5 ± 3.2 ‰ for new industrial complexes, −34.6 ± 0.4 ‰ for rural areas, and − 31.2 ± 2.6 ‰ for Lake Shihwa; Fig. 6 and Table 4). In general, the isotopic signatures of lipid compounds show evidence of ^{13}C depletion compared with bulk tissue, according to biosynthetic fractions ($\delta^{13}C_{bulk} - \delta^{13}C_{biomarker}$; 5 ‰ − 10 ‰ for algae and 7 ‰ − 10 ‰ for vascular plants; Collister et al., 1994; Ballentine et al., 1996; Schouten et al., 1998; Wiesenberg et al., 2004). In this regard, the isotopic variations of *n*-C_{27}, *n*-C_{29}, *n*-C_{31} have been typically shown for the different source origins, ranging from −37.4 ‰ to −35.6 ‰ for terrestrial C3 plants, −30.6 ‰ to −26.1 ‰ for petroleum, and − 32.2 ‰ to −31.0 ‰ for combustion, respectively (Cooper et al., 2015; O'malley et al., 1997; Wilhelms et al., 1994). Based on the results of previous studies, $\delta^{13}C$

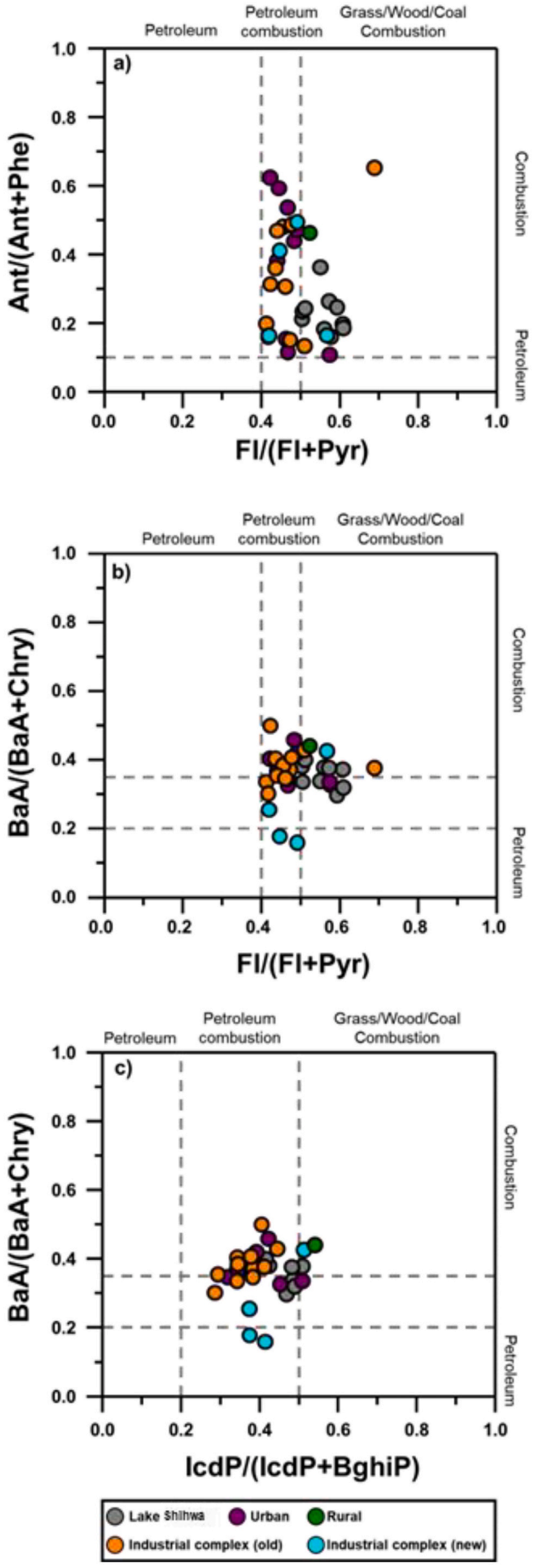

Fig. 5. Spatial variations of various PAH indices: (a) Ant/(Ant+Phe) and Fl/(Fl + Pyr) (b) BaA(BaA + Chry) and Fl/(Fl + Pyr), and (c) BaA(BaA + Chry) and IcdP/(IcdP+BghiP).

values of odd long-chain *n*-alkanes investigated at our study sites may provide evidence for the discriminative contribution of mixed OM transported from different land-use types. First, the $\delta^{13}C$ value of odd-chain alkanes from urban areas (S1, S2, S4) and industrial complexes (I10) was −33.7 ± 0.7 ‰, indicating that the deposited OM may be mixed between natural (e.g., terrestrial C3 plant) and anthropogenic (e.g. oil spill, asphalt sweeps, crankcase oil) origins (O'malley et al., 1997; Wilhelms et al., 1994; Kim et al., 2018). Second, for rural boundaries (R1), the average $\delta^{13}C$ value of odd-chain alkanes was −34.6 ± 0.5 ‰, reflecting the predominant occurrence of natural OM (e.g., tree, graminoid debris) near agriculture and forests. Given the isotopic variation in long-chain *n*-alkanes depends on multiple factors, such as source origins, physiological responses, and degradation (Farquhar et al., 1982; Meyers, 2003; Cooper et al., 2015; Kim et al., 2018), their isotopic properties within different land-use types may determine discriminative OM contributions between anthropogenic and natural origins. Based on this information, $\delta^{13}C$ values of odd-chain alkanes at Lake Shihwa (L1 − L10) showed ranges similar to those of urban and industrial boundaries. We therefore inferred that anthropogenically derived OM (e.g., from petroleum and combustion) within urban and industrial complexes are mainly deposited into the surface sediment of Lake Shihwa.

The $\delta^{13}C$ values of specific PAHs (Fl, Pyr, BaA, Chry, IcdP, BghiP) varied from −27.4 ‰ to −24.3 ‰ for urban areas, −26.9 ‰ to −24.5 ‰ for old industrial complexes, −29.4 ‰ to −26.2 ‰ for new industrial complexes, −30.3 ‰ to −26.4 ‰ for rural areas, and − 30.8 ‰ to −24.2 ‰ for Lake Shihwa (Fig. 6). Overall, $\delta^{13}C$ values of specific PAHs showed more enriched patterns, compared with those of odd long-chain *n*-alkanes (Fig. 6). Isotopic variations of specific PAHs are typically shown for different source origins (terrestrial C_3 plants: −30.0 ‰ to −27.0 ‰; petroleum: −27.3 ‰ to −26.9 ‰; and combustion: −25.6 ‰ to −21.0 ‰; Abrajano Jr. et al., 2003; Andrusevich et al., 1998; Gao et al., 2018; McRae et al., 1999; O'malley et al., 1994; Peng et al., 2006). These isotopic variations may be closely associated with the degree of the polyaromatization reactions that can cause carbon-isotopic fractionation (Bosch et al., 2015; Pedentchouk and Turich, 2018). For this study, overall $\delta^{13}C_{PAHs}$ values show overlapping isotopic patterns among different land use types (Fig. 6). However, $\delta^{13}C_{BaA+Chry}$ values at Lake Shihwa (L5, L9) and rural areas (R1) showed relatively depleted patterns (−30.4 ± 0.3 ‰), implying the partial contribution of combustion of fossil fuels. Meanwhile, the high TOC content at old industrial complexes (I4) may be influenced by anthropogenic activities, the isotopic values of specific PAHs (BaA + Chry; −26.9 ± 0.4 ‰) at this site may reflect the predominant contribution of petrogenic OM derived from urbanization and industrialization. In addition, the enrichment of $\delta^{13}C_{Pyr}$ values (−25.8 ± 0.2 ‰) also provides evidence for the petrogenic origins of OM from urban areas and old industrial complexes (O'malley et al., 1994; Abrajano Jr. et al., 2003). Combined with the evidence inferred from bulk elements and specific indices, our CSIA results suggest that anthropogenic activities near urban and industrial complexes may mainly result in a substantial increase of anthropogenic derived-OM (e.g., petroleum and combustion) within the Lake Shihwa.

3.4. Quantitative estimation of mixed OM within watersheds

The relative contribution of mixed OMs within five boundaries (Lake Shihwa, urban areas, industrial complexes, and rural areas) were estimated using a Bayesian mixing model, based on the isotopic compositions of long-chain *n*-alkanes and LMW/HMW PAHs. We used natural and anthropogenic OM end members (terrestrial C3 plants, petroleum, and combustion; Fig. 6) which have been reported near various aquatic systems (e.g., East China Sea, Bohai Bay) including those on Korean

(caption on next column)

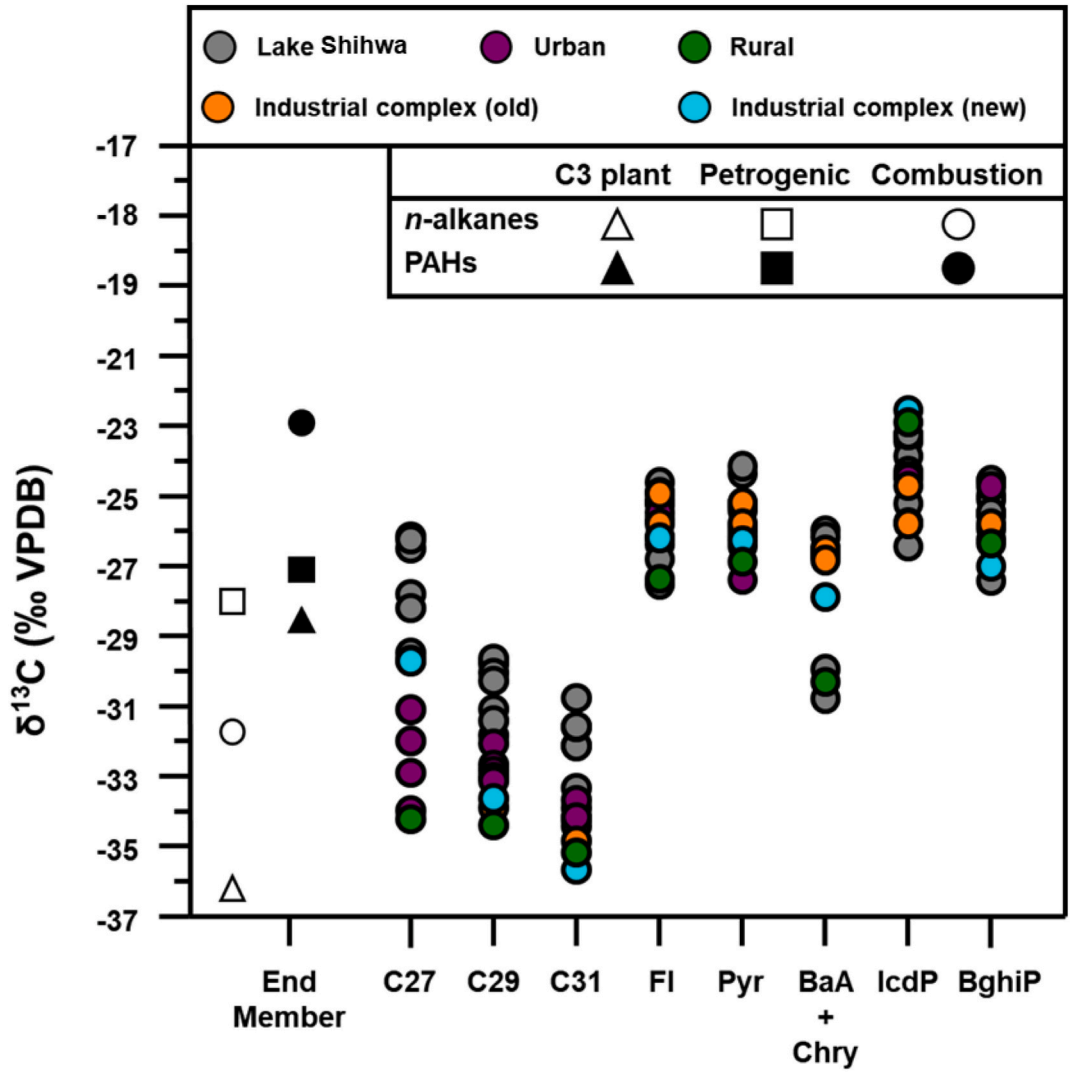

Fig. 6. Carbon isotopic compositions of specific lipid compounds ($\delta^{13}C_{C27}$, $\delta^{13}C_{C29}$, $\delta^{13}C_{C31}$, $\delta^{13}C_{Fl}$, $\delta^{13}C_{Pyr}$, $\delta^{13}C_{BaA+Chry}$, $\delta^{13}C_{Icdp}$, $\delta^{13}C_{BghiP}$).

coasts (Derrien et al., 2018; Hu et al., 2012; Wang et al., 2015). The relative contributions of three OM sources showed discriminative proportions along different land-use types of Lake Shihwa (Fig. 7 and Table 5). However, considering the transport of mixed OMs within Lake Shihwa is fluctuates drastically in tributaries (Kim et al., 2014; Lee et al., 2017b), these properties may lead to attenuated input of anthropogenic OM sources transported from industrial complex and urban. Our complementary approach involved quantitative source apportionments of mixed OM; the results were integrated into TOC abundances at five boundaries. As a result, the transport of OM from three sources showed substantial differences along land-use type in the Shihwa watershed (Fig. 7). Together with the increased TOC abundance within the urban areas and Shihwa watershed, anthropogenic sources showed substantially increased transport via urban activities and petroleum combustion. As these integrated approaches have been successfully applied to estimating the quantitative contribution of OM loading within a complex river system (Lee et al., 2021), TOC-weighted source apportionments may be useful for estimating the OM ongoing (origin and transport) during high-flow conditions. We suggest that our integrated approach may be more effective in managing water and sediment quality within complex aquatic systems, where urbanization near Lake Shihwa has been actively expanded.

Overall, our case study provides potential insights into how an integrated framework incorporating various isotopic approaches can quantitatively assess OM under the pressure of increased anthropogenic conditions in complex watersheds. Nevertheless, the quantitative estimation of mixed OMs is still subject to uncertainty arising from several limiting conditions. First, the application of multi-isotope analysis (e.g., deuterium and radiocarbon) may provide additional evidence to more precisely trace sources origins (Bosch et al., 2015; Gao et al., 2018; Ren et al., 2020). Second, incorporating additional environmental factors (e.g., rainfall and irrigation) in the case study should be explored in a future study. Although these considerations may pose difficulties when applying the method to more complicated and larger river basins, a multi-isotopic approach coupled with specific lipid compounds may demonstrate the advantages quantifying the impact of anthropogenic activities on watersheds. Finally, given that heterogeneous OM abundances near anthropogenic land-use types may be influenced by waterflow simulations (Lee et al., 2021), time-series sampling campaigns may minimize this uncertainty. An automatic sampling approach may be necessary to enhance the sampling frequency at each study site. In addition, when extended to other large-scale interface regions, the uncertainty of quantitative OM estimates may be reduced by using more sampling data. Based on these considerations, we propose that our integrated framework can be supplemented to more precisely estimate quantitative OM transport between river and coastal interfaces, with systematical management for sustainable developments.

Table 4
The carbon isotopic composition of *n*-alkanes and PAHs within land-use boundaries.

Compounds		Land use type																			
		Lake Sihwa				Urban				Old industrial complex				New industrial complex				Rural			
		Min	Max	Aver	s.d	Min	Max	Aver	s.d	Min	Max	Aver	s.d	Min	Max	Aver	s.d	Min	Max	Aver	s.d
***n*-alkanes**	C16	–	–	–	–	–	–	–	–	–	–	–	–	–	–	–	–	–	–	–	–
	C17	–	–	–	–	–	–	–	–	–	–	–	–	–	–	–	–	–	–	–	–
	Pr	–	–	–	–	–	–	–	–	–	–	–	–	–	–	–	–	–	–	–	–
	C18	−32.4	−32.4	−32.4	–	–	–	–	–	−26.5	−26.5	−26.5		−29.0	−29.0	−29.0		−28.9	−28.9	−28.9	–
	Ph	–	–	–	–	–	–	–	–	–	–	–	–	–	–	–	–	–	–	–	–
	C19	−33.6	−21.8	−28.0	±4.9	−26.9	−23.6	−25.3	±2.3	−34.5	−31.0	−32.8	±2.5	−27.1	−27.1	−27.1	–	−31.2	−31.2	−31.2	–
	C20	−27.1	−22.4	−24.8	±3.3	−25.0	−25.0	−25.0	–	−30.9	−30.9	−30.9	–	−24.8	−24.8	−24.8	–	−27.1	−27.1	−27.1	–
	C21	−30.6	−23.8	−26.4	±3.7	−28.1	−28.1	−28.1	–	–	–	–	–	−24.3	−24.3	−24.3	–	−32.9	−32.9	−32.9	–
	C22	−28.6	−27.2	−27.9	±0.6	−27.0	−27.0	−27.0	–	–	–	–	–	−25.3	−25.3	−25.3	–	−29.8	−29.8	−29.8	–
	C23	−30.6	−27.0	−28.8	±1.7	−31.4	−28.1	−29.8	±2.3	–	–	–	–	–	–	–	–	−32.4	−32.4	−32.4	–
	C24	−29.6	−27.1	−28.3	±1.2	−28.2	−24.6	−26.4	±1.5	–	–	–	–	−26.6	−26.6	−26.6	–	−30.0	−30.0	−30.0	–
	C25	−37.7	−26.6	−29.5	±3.6	−33.6	−31.0	−31.9	±1.2	−36.0	−33.1	−34.6	±2.1	−30.1	−30.1	−30.1	–	−33.7	−33.7	−33.7	–
	C26	−32.1	−17.0	−28.0	±5.1	−29.6	−27.9	−28.7	±0.7	–	–	–	–	−24.6	−24.6	−24.6	–	−30.1	−30.1	−30.1	–
	C27	−35.5	−26.2	−29.4	±3.6	−34.0	−31.1	−32.5	±1.2	−39.8	−35.8	−37.8	±2.8	−29.7	−29.7	−29.7	–	−34.3	−34.3	−34.3	–
	C28	−38.5	−29.8	−33.9	±3.0	−31.7	−29.0	−30.7	±1.2	−30.4	−30.4	−30.4	–	−31.3	−31.3	−31.3	–	−32.5	−32.5	−32.5	–
	C29	−33.6	−29.7	−31.1	±1.3	−33.2	−31.4	−32.6	±0.7	−34.0	−34.0	−34.0	–	−33.6	−27.5	−30.6	±4.3	−34.4	−34.4	−34.4	–
	C30	−32.2	−25.8	−29.6	±2.4	−31.7	−29.8	−30.7	±0.7	−26.7	−26.7	−26.7	–	−35.3	−30.6	−33.0	±3.3	−35.7	−35.7	−35.7	–
	C31	−34.5	−30.8	−32.9	±1.3	−34.5	−30.7	−33.6	±1.4	−36.0	−34.9	−35.3	±0.6	−35.7	−30.9	−33.3	±3.4	−35.2	−35.2	−35.2	–
	C32	−33.6	−10.7	−26.7	±7.5	−31.5	−30.9	−31.2	±0.2	−36.1	−32.1	−34.1	±2.8	−27.2	−27.2	−27.2	–	−30.3	−30.3	−30.3	–
	C33	−32.4	−27.5	−30.6	±1.7	−33.6	−32.1	−33.1	±0.6	−34.0	−32.2	−33.2	±0.9	−32.4	−29.3	−30.9	±2.2	−32.8	−32.8	−32.8	–
	C34	−38.8	−38.8	−38.8	–	–	–	–	–	−33.5	−29.0	−31.3	±3.2	–	–	–	–	–	–	–	–
	C35	−37.3	−30.6	−33.3	±3.6	–	–	–	–	−27.7	−25.0	−26.4	±1.9	–	–	–	–	–	–	–	–
PAHs	Phe	–	–	–	–	–	–	–	–	−28.0	−28.0	−28.0	–	–	–	–	–	–	–	–	–
	Ant	–	–	–	–	–	–	–	–	−36.6	−36.6	−36.6	–	–	–	–	–	–	–	–	–
	Fl	−27.6	−26.4	−25.8	±0.9	−25.5	−24.3	−24.9	±0.8	−25.8	−24.5	−25.1	±0.7	−26.2	−26.2	−26.2	–	−27.4	−27.4	−27.4	–
	Pyr	−26.5	−24.2	−25.4	±0.7	−27.4	−25.4	−26.4	±1.4	−25.8	−25.2	−25.6	±0.3	−26.3	−26.3	−26.3	–	−26.9	−26.9	−26.9	–
	BaA + Chry	−30.8	−26.0	−27.3	±1.7	−26.9	−26.7	−26.8	±0.1	−26.9	−25.7	−26.4	±0.6	−27.9	−27.9	−27.9	–	−30.3	−30.3	−30.3	–
	BbF	−26.9	−24.7	−25.5	±0.7	−25.3	−25.2	−25.3	±0.1	−25.9	−24.2	−25.1	±0.9	−26.5	−26.5	−26.5	–	−25.5	−25.5	−25.5	–
	BaP	−25.3	−22.7	−24.2	±0.8	−25.2	−25.1	−25.2	±0.1	−27.0	−25.6	−26.1	±0.8	−26.7	−26.7	−26.7	–	−23.5	−23.5	−23.5	–
	IcdP	−30.5	−18.6	−26.8	±3.2	−26.7	−25.8	−26.3	±0.6	−25.9	−25.5	−25.7	±0.3	−29.4	−29.4	−29.4	–	−29.9	−29.9	−29.9	–
	DahA	−26.5	−23.3	−24.4	±1.1	−24.5	−23.2	−23.9	±0.9	−25.8	−24.7	−25.3	±0.8	−22.6	−22.6	−22.6	–	−22.9	−22.9	−22.9	–
	BghiP	−27.5	−24.6	−25.5	±0.8	−24.8	−24.8	−24.8	±0.0	−26.3	−25.8	−26.1	±0.4	−27.0	−27.0	−27.0	–	−26.4	−26.4	−26.4	–

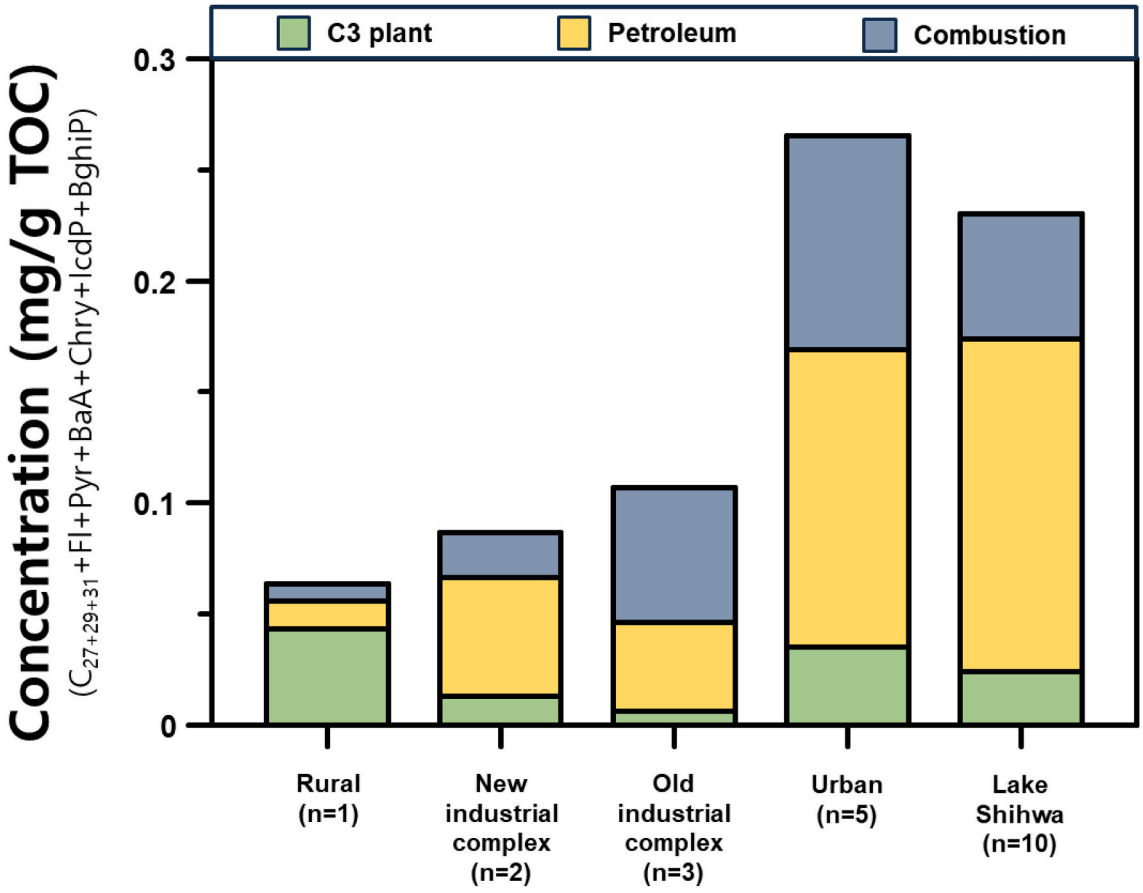

Fig. 7. Source apportionment of specific organic matter (C_3 plant, petroleum, and combustion) within five boundaries of surface sediments.

Table 5
The relative contributions of OM sources to sediment within land-use categories.

Source Land-use type	C3 plant		Petroleum		Combustion	
	Average	± Stdev	Average	± Stdev	Average	± Stdev
Rural	0.68	0.10	0.20	0.10	0.12	0.10
New industrial complex	0.15	0.07	0.62	0.11	0.23	0.10
Old industrial complex	0.06	0.04	0.37	0.10	0.57	0.11
Urban	0.13	0.09	0.51	0.15	0.36	0.16
Lake Shihwa	0.10	0.08	0.65	0.13	0.25	0.13

4. Conclusion

We tested an integrated framework using multi-isotopic properties (i.e., bulk elements and aliphatic/aromatic hydrocarbons) to effectively estimate the quantitative contribution of anthropogenic OM along different land-use types of Lake Shihwa. Together with an increased abundance of bulk elements (C; 3.4 ± 4.8 %, N; 0.8 ± 3.6 %), their isotopic compositions ($\delta^{13}C$; −24.5 ± 2.2 ‰, $\delta^{15}N$; 4.2 ± 2.7 ‰) may reflect the mixed contributions of natural and anthropogenic sources. To constrain source specificity and conservative behavior of mixed OM, we additionally investigated spatial variations in *n*-alkanes and PAHs. With respect to the predominant abundance of both hydrocarbons (*n*-alkanes; 0.2 ± 0.1 mg/g TOC and PAHs; 0.1 ± 0.3 mg/g TOC) at urban and industrial complexes, specific indices calculated via their abundances may be an indicator of mixed origins (terrestrial plants, petroleum, combustion) by various pathways (e.g., atmospheric deposition, outfall pipe, and surface runoff). Based on these properties, the compound isotopic signatures at both land-use types may provide the significant evidence for predominant anthropogenic derived-OM (> 90 %) deposited within Lake Shihwa. In the near future, assessments of water discharge, hydrological process, and multi/radioactive isotope could be tested to improve the ability to evaluate anthropogenic OM loading in other large-scale interfaces. We therefore concluded that our integrated framework can strengthen the core idea of precisely estimating quantitative OM transport between rivers and coastal interfaces.

Supplementary data to this article can be found online at https://doi.org/10.1016/j.marpolbul.2024.117220.

CRediT authorship contribution statement

Rincheon Jeon: Writing – original draft, Visualization, Methodology, Investigation, Formal analysis, Data curation. **Seung-Hee Kim:** Writing – review & editing, Visualization, Investigation, Formal analysis, Data curation, Conceptualization. **Dong-Hun Lee:** Writing – review & editing, Validation, Supervision, Resources, Funding acquisition, Data curation, Conceptualization. **Yusang Cho:** Methodology, Investigation, Formal analysis. **Youngnam Kim:** Methodology, Formal analysis, Data curation. **Seongjin Hong:** Writing – review & editing. **Kyung-Hoon Shin:** Writing – review & editing, Validation, Supervision, Project administration, Funding acquisition.

Declaration of competing interest

The authors declare that they have no competing financial interests or personal relationships that appear to influence the work reported in this paper.

Acknowledgments

This work was supported by the development of source identification and apportionment methods for toxic substances in marine environments program of the Korea Institute of Marine Science & Technology Promotion, funded by the Ministry of Oceans and Fisheries (KIMST-20220534). This work was also supported by the Global-Learning & Academic research institution for master's and PhD students and postdocs (G-LAMP) Program of the National Research Foundation of Korea grant funded by the Ministry of Education (No. RS-2023-00301702).

Data availability

Data will be made available on request.

References

Abdel-Shafy, H.I., Mansour, M.S.M., 2016. A review on polycyclic aromatic hydrocarbons: source, environmental impact, effect on human health and remediation. Egypt. J. Pet. 25 (1), 107–123.
Abrajano Jr., T.A., Yan, B., O'Malley, V., 2003. High-molecular-weight petrogenic and pyrogenic hydrocarbons in aquatic environments. Treatise on Geochemistry 9, 475–509.
Andrusevich, V.E., Engel, M.H., Zumberge, J.E., Brothers, L.A., 1998. Secular, episodic changes in stable carbon isotope composition of crude oils. Chem. Geol. 152 (1–2), 59–72.
Baek, K.M., Seo, Y.K., Kim, J.Y., Baek, S.O., 2020. Monitoring of particulate hazardous air pollutants and affecting factors in the largest industrial area in South Korea: the Sihwa-Banwol complex. Environ. Eng. Res. 25 (6), 908–923.
Ballentine, D.C., Macko, S.A., Turekian, V.C., Gilhooly, W.P., Martincigh, B., 1996. Compound specific isotope analysis of fatty acids and polycyclic aromatic hydrocarbons in aerosols: implications for biomass burning. Org. Geochem. 25 (1–2), 97–104.
Bauer, J.E., Cai, W.J., Raymond, P.A., Bianchi, T.S., Hopkinson, C.S., Regnier, P.A.G., 2013. The changing carbon cycle of the coastal ocean. Nature 504 (7478), 61–70.
Bian, Q., Alharbi, B., Collett Jr., J., Kreidenweis, S., Pasha, M.J., 2016. Measurements and source apportionment of particle-associated polycyclic aromatic hydrocarbons in ambient air in Riyadh, Saudi Arabia. Atmos. Environ. 137, 186–198.
Bianchi, T.S., Mitra, S., McKee, B.A., 2002. Sources of terrestrially-derived organic carbon in lower Mississippi River and Louisiana shelf sediments: implications for differential sedimentation and transport at the coastal margin. Mar. Chem. 77 (2–3), 211–223.
Bosch, C., Andersson, A., Kruså, M., Bandh, C., Hovorková, I., Klánová, J., Knowles, T.D. J., Pancost, R.D., Evershed, R.P., Gustafsson, Ö., 2015. Source apportionment of polycyclic aromatic hydrocarbons in central European soils with compound-specific triple isotopes ($\delta^{13}C$, $\Delta^{14}C$, and $\delta^{2}H$). Environ. Sci. Technol. 49 (13), 7657–7665.
Bottchew, J., Strebel, O., Voerkelius, S., Schmidt, H.-L., 1990. Using isotope fractionation of nitrate-nitrogen and nitrate-oxygen for evaluation of microbial denitrification in a sandy aquifer. J. Hydrol. 114 (3–4), 413–424.
Bourbonniere, R.A., Meyers, P.A., 1996. Sedimentary geolipid records of historical changes in the watersheds and productivities of Lakes Ontario and Erie. Limnol. Oceanogr. 41 (2), 352–359.
Bouwman, A.F., Bierkens, M.F.P., Griffioen, J., Hefting, M.M., Middelburg, J.J., Middelkoop, H., Slomp, C.P., 2013. Nutrient dynamics, transfer and retention along the aquatic continuum from land to ocean: towards integration of ecological and biogeochemical models. Biogeosciences 10 (1), 1–22.
Bray, E.E., Evans, E.D., 1961. Distribution of n-paraffins as a clue to recognition of sources beds. Geochim. Cosmochim. Acta 22 (1), 2–15.
Bush, R.T., McInerney, F.A., 2013. Leaf wax n-alkane distributions in and across modern plants: implications for paleoecology and chemotaxonomy. Geochim. Cosmochim. Acta 117, 161–179.
Canuel, E.A., Hardison, A.K., 2016. Sources, ages, and alteration of organic matter in estuaries. Annu. Rev. Mar. Sci. 8, 409–434.
Canuel, E.A., Freeman, K.H., Wakeham, S.G., 1997. Isotopic compositions of lipid biomarker compounds in estuarine plants and surface sediments. Limnol. Oceanogr. 42 (7), 1570–1583.
Chen, X., Seo, H., Han, H., Seo, J., Kim, T., Kim, G., 2021. Conservative behavior of terrestrial trace elements associated with humic substances in the coastal ocean. Geochim. Cosmochim. Acta 308, 373–383.
Chikaraishi, Y., Naraoka, H., Poulson, S.R., 2004. Hydrogen and carbon isotopic fractionations of lipid biosynthesis among terrestrial (C3, C4 and CAM) and aquatic plants. Phytochemistry 65 (10), 1369–1381.
Cloern, J.E., Canuel, E.A., Harris, D., 2002. Stable carbon and nitrogen isotope composition of aquatic and terrestrial plants of the San Francisco Bay estuarine system. Limnol. Oceanogr. 47 (3), 713–729.
Collister, J.W., Rieley, G., Stern, B., Eglinton, G., Fry, B., 1994. Compound-specific δ13C analyses of leaf lipids from plants with differing carbon dioxide metabolisms. Org. Geochem. 21 (6–7), 619–627.
Colombo, J.C., Pelletier, E., Brochu, C., Khalil, M., Catogglo, J.A., 1989. Determination of hydrocarbon sources using n-alkane and polyaromatic hydrocarbon distribution indexes. Case study: Rio de la Plata estuary, Argentina. Environ. Sci. Technol. 23 (7), 888–894.
Conesa, J.A., Nuñez, S.S., Ortuño, N., Moltó, J., 2021. Pah and pop presence in plastic waste and recyclates: state of the art. Energies 14 (12).
Cooper, R.J., Pedentchouk, N., Hiscock, K.M., Disdle, P., Krueger, T., Rawlins, B.G., 2015. Apportioning sources of organic matter in streambed sediments: an integrated molecular and compound-specific stable isotope approach. Sci. Total Environ. 520, 187–197.
Cranwell, I.P.A., Eglinton, G., Robinson, N., 1987. Lipids of aquatic organisms as potential contributors to lacustrine sediments—II. Org. Geochem. 11 (6), 513–527.
Dai, C., Han, Y., Duan, Y., Lai, X., Fu, R., Liu, S., Zhou, L., 2022. Review on the contamination and remediation of polycyclic aromatic hydrocarbons (PAHs) in coastal soil and sediments. Environ. Res. 205, 112423.
Debruyn, A.M.H., Rasmussen, J.B., 2002. Quantifying assimilation of sewage-derived organic matter by riverine benthos. Ecol. Appl. 12 (2), 511–520.
Derrien, M., Kim, M.S., Ock, G., Hong, S., Cho, J., Shin, K.H., Hur, J., 2018. Estimation of different source contributions to sediment organic matter in an agricultural-forested watershed using end member mixing analyses based on stable isotope ratios and fluorescence spectroscopy. Sci. Total Environ. 618, 569–578.
Diebel, M.W., Jake, A.M., Zanden, V., 2009. Nitrogen stable isotopes in streams: effects of agricultural sources and transformations. Ecol. Appl. 19 (5), 1127–1134.
Divers, M.T., Elliott, E.M., Bain, D.J., 2014. Quantification of nitrate sources to an urban stream using dual nitrate isotopes. Environ. Sci. Technol. 48 (18), 10580–10587.
Dover, C.L.v, Grassle, J.F., Fry, B., Garritt, R.H., Starczak, V.R., 1992. Stable isotope evidence for entry of sewage-derived organic material into a deep-sea food web. Nature 360 (6400), 153–156.
Dvorská, A., Lammel, G., Klánová, J., 2011. Use of diagnostic ratios for studying source apportionment and reactivity of ambient polycyclic aromatic hydrocarbons over Central Europe. Atmos. Environ. 45 (2), 420–427.
Elliott, E.M., Brush, G.S., 2006. Sedimented organic nitrogen isotopes in freshwater wetlands record long-term changes in watershed nitrogen source and land use. Environ. Sci. Technol. 40 (9), 2910–2916.
Farquhar, G.D., O'Leary, M.H., Berry, J.A., 1982. On the relationship between carbon isotope discrimination and the intercellular carbon dioxide concentration in leaves. Funct. Plant Biol. 9 (2), 121–137.
Ficken, K.J., Li, B., Swain, D.L., Eglinton, G., 2000. An n-alkane proxy for the sedimentary input of submerged/floating freshwater aquatic macrophytes. Org. Geochem. 31 (7–8), 745–749.
Fry, B., 2006. Using stable isotope tracers. Stable isotope ecology 40–75.
Fry, B., Sherr, E.B., 1989. $\delta^{13}C$ measurements as indicators of carbon flow in marine and freshwater ecosystems. In: Stable Isotopes in Ecological Research, pp. 196–229.
Galarneau, E., 2008. Source specificity and atmospheric processing of airborne PAHs: implications for source apportionment. Atmos. Environ. 42 (35), 8139–8149.
Gao, X., Yang, Y., Wang, C., 2012. Geochemistry of organic carbon and nitrogen in surface sediments of coastal Bohai Bay inferred from their ratios and stable isotopic signatures. Mar. Pollut. Bull. 64 (6), 1148–1155.
Gao, P., Li, H., Wilson, C.P., Townsend, T.G., Xiang, P., Liu, Y., Ma, L.Q., 2018. Source identification of PAHs in soils based on stable carbon isotopic signatures. Crit. Rev. Environ. Sci. Technol. 48 (13–15), 923–948.
Gelpi, E., Schneider, H., Mann, J., Oro, J., 1970. Hydrocarbons of geochemical significance in microscopic algae. Phytochemistry 9 (3), 603–612.
Gleason, J.D., Kyser, T.K., 1984. Stable isotope compositions of gases and vegetation. Nature 307, 254–257.
Grimmer, G., Jacob, J., Naujack, K.-W., 1981. Profile of the polycyclic aromatic hydrocarbons from lubricating oils inventory by GCGC/MS-PAH in environmental materials, part 1 *. Anal. Chem. 309, 13–19.
Grimmer, G., Jacob, J., Naujack, K.-W., 1983. Profile of the polycyclic aromatic compounds from crude oils. Fresenius' Zeitschrift Fuer Analytische Chemie 314 (1), 29–36.
Gschwend, P.M., Hites, R.A., 1981. Fluxes of polycyclic aromatic hydrocarbons to marine and lacustrine sediments in the northeastern United States. Geochim. Cosmochim. Acta 45 (12), 2359–2367.
Gu, B., Chapman, A.D., Schelske, C.L., 2006. Factors controlling seasonal variations in stable isotope composition of particulate organic matter in a softwater eutrophic lake. Limnol. Oceanogr. 51 (6), 2837–2848.
Hedges, J.I., Keil, R.G., 1995. Sedimentary organic matter preservation: an assessment and speculative synthesis. Mar. Chem. 49 (2–3), 81–115.
Hedges, J.I., Oades, J.M., 1997. Comparative organic geochemistries of soils and marine sediments. Org. Geochem. 27 (7–8), 319–361.
Hedges, J.I., Clark, W.A., Cowie, G.L., 1988. Organic matter sources to the water column and surficial sediments of a marine bay. Limnol. Oceanogr. 33 (5), 1116–1136.
Hong, S., Lee, Y., Yoon, S.J., Lee, J., Kang, S., Won, E.J., Hur, J., Khim, J.S., Shin, K.H., 2019. Carbon and nitrogen stable isotope signatures linked to anthropogenic toxic substances pollution in a highly industrialized area of South Korea. Mar. Pollut. Bull. 144, 152–159.
Howarth, R.W., 2008. Coastal nitrogen pollution: coastal nitrogen pollution: a review of sources and trends globally and regionally. Harmful Algae 8 (1), 14–20.

Hu, J., Jia, G., Mai, B., Zhang, G., 2006. Distribution and sources of organic carbon, nitrogen and their isotopes in sediments of the subtropical Pearl River estuary and adjacent shelf, Southern China. Mar. Chem. 98 (2–4), 274–285.
Hu, L., Shi, X., Yu, Z., Lin, T., Wang, H., Ma, D., Guo, Z., Yang, Z., 2012. Distribution of sedimentary organic matter in estuarine–inner shelf regions of the East China Sea: implications for hydrodynamic forces and anthropogenic impact. Mar. Chem. 142, 29–40.
Inomura, K., Deutsch, C., Jahn, O., Dutkiewicz, S., Follows, M.J., 2022. Global patterns in marine organic matter stoichiometry driven by phytoplankton ecophysiology. Nat. Geosci. 15 (12), 1034–1040.
Jenkins, B.M., Jones, A.D., Turn, S.Q., Williams, R.B., 1996. Emission factors for polycyclic aromatic hydrocarbons from biomass burning. Environ. Sci. Technol. 30 (8), 2462–2469.
Kang, M., Kim, K., Choi, N., Kim, Y.P., Lee, J.Y., 2020. Recent occurrence of PAHs and n-alkanes in pm2.5 in Seoul, Korea and characteristics of their sources and toxicity. Int. J. Environ. Res. Public Health 17 (4).
Kelly, B.C., Ikonomou, M.G., Blair, J.D., Morin, A.E., Gobas, F.A.P.C., 2007. Food web specific biomagnification of persistent organic pollutants. Science 317 (5835), 236–239.
Khim, J.S., Villeneuve, D.L., Kannan, K., Lee, K.T., Snyder, S.A., Koh, C.H., Giesy, J.P., 1999. Alkylphenols, polycyclic aromatic hydrocarbons, and organochlorines in sediment from Lake Shihwa, Korea: instrumental and bioanalytical characterization. Environ. Toxicol. Chem. 18 (11), 2424–2432.
Kim, S.K., Chae, D.H., 2016. Seasonal variation in diffusive exchange of polycyclic aromatic hydrocarbons across the air–seawater interface in coastal urban area. Mar. Pollut. Bull. 109 (1), 221–229.
Kim, S.W., Park, J.S., Kim, D., Oh, J.M., 2014. Runoff characteristics of non-point pollutants caused by different land uses and a spatial overlay analysis with spatial distribution of industrial cluster: a case study of the Lake Sihwa watershed. Environ. Earth Sci. 71 (1), 483–496.
Kim, M.S., Lee, W.S., Suresh Kumar, K., Shin, K.H., Robarge, W., Kim, M., Lee, S.R., 2016. Effects of HCl pretreatment, drying, and storage on the stable isotope ratios of soil and sediment samples. Rapid Commun. Mass Spectrom. 1567–1575.
Kim, J.-H., Lee, D.-H., Yoon, S.H., Jeong, K.S., Choi, B., Shin, K.-H., 2017. Contribution of petroleum-derived organic carbon to sedimentary organic carbon pool in the eastern Yellow Sea (the northwestern Pacific). Chemosphere 168, 1389–1399.
Kim, D., Kim, J.H., Kim, M.S., Ra, K., Shin, K.H., 2018. Assessing environmental changes in Lake Shihwa, South Korea, based on distributions and stable carbon isotopic compositions of n-alkanes. Environ. Pollut. 240, 105–115.
Kim, M.-J., Baek, K.-M., Heo, J.-B., Cheong, J.-P., Baek, S.-O., 2021. Concentrations, health risks, and sources of hazardous air pollutants in Seoul-Incheon, a megacity area in Korea. Air Qual. Atmos. Health 14 (6), 873–893.
Kim, C.-S., Kim, S.-H., Lee, W.C., Lee, D.-H., 2022. Spatial variability of water quality and sedimentary organic matter during winter season in coastal aquaculture zone of Korea. Mar. Pollut. Bull. 182, 113991.
Kim, M.S., Lim, B.R., Jeon, P., Hong, S., Jeon, D., Park, S.Y., Hong, S., Yoo, E.J., Kim, H. S., Shin, S., Yoon, J. ki, 2023. Innovative approach to reveal source contribution of dissolved organic matter in a complex river watershed using end-member mixing analysis based on spectroscopic proxies and multi-isotopes. Water Res. 230.
Kim, S.H., Kim, M.S., Lee, D.H., Shin, K.H., 2024. Impact of typhoons on anthropogenic nitrogen sources in Lake Sihwa, South Korea. Mar. Pollut. Bull. 202, 116324.
Kwon, H.O., Choi, S.D., 2014. Polycyclic aromatic hydrocarbons (PAHs) in soils from a multi-industrial city, South Korea. Sci. Total Environ. 470, 1494–1501.
Laflamme, R.E., Hites, R.A., 1978. The global distribution of polycyclic aromatic hydrocarbons in recent sediments. Geochim. Cosmochim. Acta 42 (3), 289–303.
Lee, Y., Hur, J., Shin, K.H., 2014. Characterization and source identification of organic matter in view of land uses and heavy rainfall in the Lake Shihwa, Korea. Mar. Pollut. Bull. 84 (1–2), 322–329.
Lee, J., Hong, S., Yoon, S.J., Kwon, B.O., Ryu, J., Giesy, J.P., Allam, A.A., Al-khedhairy, A.A., Khim, J.S., 2017a. Long-term changes in distributions of dioxin-like and estrogenic compounds in sediments of Lake Sihwa, Korea: revisited mass balance. Chemosphere 181, 767–777.
Lee, Y., Hong, S., Kim, M.S., Kim, D., Choi, B.H., Hur, J., Khim, J.S., Shin, K.H., 2017b. Identification of sources and seasonal variability of organic matter in Lake Sihwa and surrounding inland creeks, South Korea. Chemosphere 177, 109–119.
Lee, J., Park, K.T., Lim, J.H., Yoon, J.E., Kim, I.N., 2018a. Hypoxia in Korean coastal waters: a case study of the natural Jinhae Bay and artificial Shihwa Bay. Front. Mar. Sci. 5, 70.
Lee, S., Cho, H.J., Choi, W., Moon, H.B., 2018b. Organophosphate flame retardants (OPFRs) in water and sediment: occurrence, distribution, and hotspots of contamination of Lake Shihwa, Korea. Mar. Pollut. Bull. 130, 105–112.
Lee, D.H., Kim, S.H., Won, E.J., Kim, M.S., Hur, J., Shin, K.H., 2021. Integrated approach for quantitative estimation of particulate organic carbon sources in a complex river system. Water Res. 199, 117194.
Li, X., Ding, Y., Han, T., Xu, J., Kang, S., Wu, Q., Sillanpaa, M., Yu, Z., Yu, C., 2017. Seasonal variations of organic carbon and nitrogen in the upper basins of Yangtze and Yellow Rivers. J. Mt. Sci. 14, 1577–1590.
Li, Y., Liu, M., Hou, L., Li, X., Yin, G., Sun, P., Yang, J., Wei, X., He, Y., Zheng, D., 2021. Geographical distribution of polycyclic aromatic hydrocarbons in estuarine sediments over China: human impacts and source apportionment. Sci. Total Environ. 768, 145279.
Liu, J., Zhao, S., Zhang, R., Dai, Y., Zhang, C., Jia, H., Guo, X., 2021. How important is abiotic dissipation in natural attenuation of polycyclic aromatic hydrocarbons in soil? Sci. Total Environ. 758, 143687.
Maksymowska, D., Richard, P., Piekarek-Jankowska, H., Riera, P., 2000. Chemical and isotopic composition of the organic matter sources in the Gulf of Gdansk (Southern Baltic Sea). Estuar. Coast. Shelf Sci. 51 (5), 585–598.
Maletić, S.P., Beljin, J.M., Rončević, S.D., Grgić, M.G., Dalmacija, B.D., 2019. State of the art and future challenges for polycyclic aromatic hydrocarbons is sediments: sources, fate, bioavailability and remediation techniques. J. Hazard. Mater. 365, 467–482.
Marshall, C.P., Love, G.D., Snape, C.E., Hill, A.C., Allwood, A.C., Walter, M.R., van Kranendonk, M.J., Bowden, S.A., Sylva, S.P., Summons, R.E., 2007. Structural characterization of kerogen in 3.4 Ga Archaean cherts from the Pilbara Craton, Western Australia. Precambrian Res. 155 (1–2), 1–23.
Martinelli, G., Dadomo, A., de Luca, D.A., Mazzola, M., Lasagna, M., Pennisi, M., Pilla, G., Sacchi, E., Saccon, P., 2018. Nitrate sources, accumulation and reduction in groundwater from Northern Italy: insights provided by a nitrate and boron isotopic database. Appl. Geochem. 91 (January), 23–35.
McRae, C., Sun, C.-G., Snape, C.E., Fallick, A.E., Taylor, D., 1999. δ13C values of coal-derived PAHs from different processes and their application to source apportionment. Org. Geochem. 30 (8), 881–889.
Mead, R., Xu, Y., Chong, J., Jaffé, R., 2005. Sediment and soil organic matter source assessment as revealed by the molecular distribution and carbon isotopic composition of n-alkanes. Org. Geochem. 36 (3), 363–370.
Medeiros, P.M., Bícego, M.C., Castelao, R.M., del Rosso, C., Fillmann, G., Zamboni, A.J., 2005. Natural and anthropogenic hydrocarbon inputs to sediments of Patos Lagoon Estuary, Brazil. Environ. Int. 31 (1), 77–87.
Meyers, P.A., 1997. Organic geochemical proxies of palaeoceanographic, paleolimnologic, and paleoclimatic processes. Org. Geochem. 27 (5–6), 213–250.
Meyers, P.A., 2003. Applications of organic geochemistry to paleolimnological reconstructions: a summary of examples from the Laurentian Great Lakes. Org. Geochem. 34 (2), 261–289.
Mille, G., Asia, L., Guiliano, M., Malleret, L., Doumenq, P., 2007. Hydrocarbons in coastal sediments from the Mediterranean Sea (Gulf of Fos area, France). Mar. Pollut. Bull. 54 (5), 566–575.
Ministry of maritime affairs and fisheries (MOMAF), 2011. The Lake Shihwa Coastal Environment Management.
Moon, H.B., Choi, M., Choi, H.G., Kannan, K., 2012. Severe pollution of PCDD/Fs and dioxin-like PCBs in sediments from Lake Shihwa, Korea: tracking the source. Mar. Pollut. Bull. 64 (11), 2357–2363.
Newbold, T., Hudson, L.N., Hill, S.L.L., Contu, S., Lysenko, I., Senior, R.A., Börger, L., Bennett, D.J., Choimes, A., Collen, B., Day, J., de Palma, A., Díaz, S., Echeverria-Londoño, S., Edgar, M.J., Feldman, A., Garon, M., Harrison, M.L.K., Alhusseini, T., Ingram, D.J., Itescu, Y., Kattge, J., Kemp, V., Kirkpatrick, L., Kleyer, M., Correia, D.L. P., Martin, C.D., Meiri, S., Novosolov, M., Pan, Y., Phillips, H.R.P., Purves, D.W., Robinson, A., Simpson, J., Tuck, S.L., Weiher, E., White, H.J., Ewers, R.M., MacE, G. M., Scharlemann, J.P.W., Purvis, A., 2015. Global effects of land use on local terrestrial biodiversity. Nature 520 (7545), 45–50.
Ogrinc, N., Fontolan, G., Faganeli, J., Covelli, S., 2005. Carbon and nitrogen isotope compositions of organic matter in coastal marine sediments (the Gulf of Trieste, N Adriatic Sea): indicators of sources and preservation. Mar. Chem. 95 (3–4), 163–181.
Oh, S., Kim, M.K., Yi, S.M., Zoh, K.D., 2010. Distributions of total mercury and methylmercury in surface sediments and fishes in Lake Shihwa, Korea. Sci. Total Environ. 408 (5), 1059–1068.
Ohkouchi, N., Takano, Y., 2013. Organic nitrogen: sources, fates, and chemistry. Treatise on geochemistry 2, 251–289.
Okuda, T., Takada, H., Naraoka, H., 2003. Thermodynamic behavior of stable carbon isotopic compositions of individual polycyclic aromatic hydrocarbons derived from automobiles. Polycycl. Aromat. Compd. 23 (2), 219–236.
O'malley, V.P., Jr, T.A.A, Hellou, J., 1994. Determination of the 13C12c ratios of individual PAH from environmental samples: can PAH sources be apportioned? Org. Geochem. 21 (6–7), 809–822.
O'malley, V.P., Burke, R.A., Schlotzhauer, W.S., 1997. Using GC–MS/combustion/IRMS to determine the 13C/12C ratios of individual hydrocarbons produced from the combustion of biomass materials—application to biomass burning. Org. Geochem. 27 (7–8), 567–581.
Oros, D.R., Simoneit, B.R.T., 2000. Identification and emission rates of molecular tracers in coal smoke particulate matter. Fuel 79 (5), 515–536.
Ortiz, J.E., Moreno, L., Torres, T., Vegas, J., Ruiz-Zapata, B., García-Cortés, Á., Galán, L., Pérez-González, A., 2013. A 220 ka paleoenvironmental reconstruction of the Fuentillejo maar lake record (Central Spain) using biomarker analysis. Org. Geochem. 55, 85–97.
Parat, C., Leveque, J., Chaussod, R., Andreux, F., 2007. Sludge-derived organic carbon in an agricultural soil estimated by 13C abundance measurements. Eur. J. Soil Sci. 58 (1), 166–173.
Parnell, A.C., Phillips, D.L., Bearhop, S., Semmens, B.X., Ward, E.J., Moore, J.W., Jackson, A.L., Grey, J., Kelly, D.J., Inger, R., 2013. Bayesian stable isotope mixing models. Environmetrics 24 (6), 387–399.
Pedentchouk, N., Turich, C., 2018. Carbon and hydrogen isotopic compositions of n-alkanes as a tool in petroleum exploration. Geol. Soc. Lond. Spec. Publ. 468 (1), 105–125.
Pedrosa-Pàmies, R., Parinos, C., Sanchez-Vidal, A., Gogou, A., Calafat, A., Canals, M., Bouloubassi, I., Lampadariou, N., 2015. Composition and sources of sedimentary organic matter in the deep eastern Mediterranean Sea. Biogeosciences 12 (24), 7379–7402.
Peng, L., You, Y., Bai, Z., Zhu, T., Xie, K., Feng, Y.-C., Li, Z., 2006. Stable carbon isotope evidence for origin of atmospheric polycyclic aromatic hydrocarbons in Zhengzhou and Urumchi, China. Geochem. J. 40 (3), 219–226.
Peters, K.E., Walters, C.C., Moldowan, J.M., 2007. The Biomarker Guide, Second edition 1.

Poynter, J., Eglinton, G., 1991. The biomarker concept—strengths and weaknesses. Fresenius J. Anal. Chem. 339 (10), 725–731.
Ra, K., Bang, J.H., Lee, J.M., Kim, K.T., Kim, E.S., 2011. The extent and historical trend of metal pollution recorded in core sediments from the artificial Lake Shihwa, Korea. Mar. Pollut. Bull. 62 (8), 1814–1821.
Ramaswamy, V., Gaye, B., Shirodkar, P.v, Rao, P.S., Chivas, A.R., Wheeler, D., Thwin, S., 2008. Distribution and sources of organic carbon, nitrogen and their isotopic signatures in sediments from the Ayeyarwady (Irrawaddy) continental shelf, northern Andaman Sea. Mar. Chem. 111 (3–4), 137–150.
Ren, L., Ren, L., Wang, Y., Wang, Y., Kawamura, K., Bikkina, S., Haghipour, N., Haghipour, N., Wacker, L., Pavuluri, C.M., Zhang, Z., Yue, S., Yue, S., Sun, Y., Wang, Z., Zhang, Y., Feng, X., Liu, C.Q., Eglinton, T.I., Fu, P., 2020. Source forensics of n-alkanes and n-fatty acids in urban aerosols using compound specific radiocarbon/stable carbon isotopic composition. Environ. Res. Lett. 15 (7), 074007.
Rojo, F., 2009. Degradation of alkanes by bacteria. Environ. Microbiol. 11 (10), 2477–2490.
Rostkowski, P., Yamashita, N., Man So, I.K., Taniyasu, S., Kwan Sing Lam, P., Falandysz, J., Tae Lee, K., Kyu Kim, S., Seong Khim, J., Hyeon, S.I., Newsted, J.L., Jones, P.D., Kannan, K., Giesy, J.P., 2006. Perfluorinated compounds in streams of the Shihwa industrial zone and Lake Shihwa, South Korea. Environ. Toxicol. Chem. 25 (9), 2374–2380.
Ryu, H.D., Kim, S.J., Baek, U. il, Kim, D.W., Lee, H.J., Chung, E.G., Kim, M.S., Kim, K., Lee, J.K., 2021. Identifying nitrogen sources in intensive livestock farming watershed with swine excreta treatment facility using dual ammonium ($\delta^{15}N_{NH4}$) and nitrate ($\delta^{15}N_{NO3}$) nitrogen isotope ratios axes. Sci. Total Environ. 779, 146480.
Saintilan, N., Rogers, K., Mazumder, D., Woodroffe, C., 2013. Allochthonous and autochthonous contributions to carbon accumulation and carbon store in southeastern Australian coastal wetlands. Estuar. Coast. Shelf Sci. 128, 84–92.
Sarma, V.V.S.S., Krishna, M.S., Prasad, V.R., Kumar, B.S.K., Naidu, S.A., Rao, G.D., Viswanadham, R., Sridevi, T., Kumar, P.P., Reddy, N.P.C., 2014. Distribution and sources of particulate organic matter in the Indian monsoonal estuaries during monsoon. J. Geophys. Res. Biogeosci. 119 (11), 2095–2111.
Schouten, S., Klein Breteler, W.C.M., Blokker, P., Schogt, N., Irene, W., Rijpstra, C., Grice, K., Baas, M., Sinninghe Damsté, J.S., 1998. Biosynthetic effects on the stable carbon isotopic compositions of algal lipids: implications for deciphering the carbon isotopic biomarker record. Geochim. Cosmochim. Acta 62 (8), 1397–1406.
Sikes, E.L., Uhle, M.E., Nodder, S.D., Howard, M.E., 2009. Sources of organic matter in a coastal marine environment: evidence from n-alkanes and their $\delta^{13}C$ distributions in the Hauraki Gulf, New Zealand. Mar. Chem. 113 (3–4), 149–163.
Silliman, J.E., Meyers, P.A., Bourbonniere, R.A., 1996. Record of postglacial organic matter delivery and burial in sediments of Lake Ontario. Org. Geochem. 24 (4), 463–472.
Smith, B.N., Epstein, S., 1971. Two categories of $^{13}C/^{12}C$ ratios for higher plants. Plant Physiol. 47 (3), 380–384.
Smith, V.H., Tilman, G.D., Nekola, J.C., 1999. Eutrophication: impacts of excess nutrient inputs on freshwater, marine, and terrestrial ecosystems. Environ. Pollut. 100 (1–3), 179–196.
Sojinu, S.O., Sonibare, O.O., Ekundayo, O., Zeng, E.Y., 2012. Assessing anthropogenic contamination in surface sediments of Niger Delta, Nigeria with fecal sterols and n-alkanes as indicators. Sci. Total Environ. 441, 89–96.
Spies, R.B., Kruger, H., Ireland, R., Rice, D.W., 1989. Stable isotope ratios and contaminant concentrations in a sewage-distorted food web. Mar. Ecol.-Prog. Ser. 157–170.
Stogiannidis, E., Laane, R., 2015. Source characterization of polycyclic aromatic hydrocarbons by using their molecular indices: an overview of possibilities. Rev. Environ. Contam. Toxicol. 49–133.
Tareq, S.M., Tanoue, E., Tsuji, H., Tanaka, N., Ohta, K., 2005. Hydrocarbon and elemental carbon signatures in a tropical wetland: biogeochemical evidence of forest fire and vegetation changes. Chemosphere 59 (11), 1655–1665.
Thornton, S.F., McManus, J., 1994. Application of organic carbon and nitrogen stable isotope and C/N ratios as source indicators of organic matter provenance in estuarine systems: evidence from the Tay Estuary, Scotland. Estuar. Coast. Shelf Sci. 38 (3), 219–233.
Tobiszewski, M., Namieśnik, J., 2012. PAH diagnostic ratios for the identification of pollution emission sources. Environ. Pollut. 162, 110–119.
Van der Oost, R., Beyer, J., Vermeulen, N.P., 2003. Fish bioaccumulation and biomarkers in environmental risk assessment: a review. Environ. Toxicol. Pharmacol. 13 (2), 57–149.
Venturini, N., Bícego, M.C., Taniguchi, S., Sasaki, S.T., García-Rodríguez, F., Brugnoli, E., Muniz, P., 2015. A multi-molecular marker assessment of organic pollution in shore sediments from the Río de la Plata Estuary, SW Atlantic. Mar. Pollut. Bull. 91 (2), 461–475.
Vitòria, L., Otero, N., Soler, A., Canals, A., 2004. Fertilizer characterization: isotopic data (N, S, O, C, and Sr). Environ. Sci. Technol. 38 (12), 3254–3262.
Volkman, J.K., Holdsworth, D.G., Neilp, G.P., Bavor, H.J., 1992. Identification of natural, anthropogenic and petroleum hydrocarbons in aquatic sediments. Sci. Total Environ. 112 (2–3), 203–219.
Vörösmarty, C.J., McIntyre, P.B., Gessner, M.O., Dudgeon, D., Prusevich, A., Green, P., Glidden, S., Bunn, S.E., Sullivan, C.A., Liermann, C.R., Davies, P.M., 2010. Global threats to human water security and river biodiversity. Nature 467 (7315), 555–561.
Vuorio, K., Meili, M., Sarvala, J., 2006. Taxon-specific variation in the stable isotopic signatures ($\delta^{13}C$ and $\delta^{15}N$) of lake phytoplankton. Freshw. Biol. 51 (5), 807–822.
Wakeham, S.G., Schaffner, C., Gxer, W., 1980. Poly cyclic aromatic hydrocarbons in recent lake sediments—II. Compounds derived from biogenic precursors during early diagenesis. Geochim. Cosmochim. Acta 44 (3), 415–429.
Walling, D.E., 2006. Human impact on land–ocean sediment transfer by the world's rivers. Geomorphology 79 (3–4), 192–216.
Wang, Z., Fingas, M., Shu, Y.Y., Sigouin, L., Landriault, M., Lambert, P., Turpin, R., Campagna, P., Mullin, J., 1999. Quantitative characterization of PAHs in burn residue and soot samples and differentiation of pyrogenic PAHs from petrogenic PAHs– the 1994 mobile burn study. Environ. Sci. Technol. 33 (18), 3100–3109.
Wang, Yongli, Fang, X., Zhang, T., Li, Y., Wu, Y., He, D., Wang, Youxiao, 2010. Predominance of even carbon-numbered n-alkanes from lacustrine sediments in Linxia Basin, NE Tibetan Plateau: implications for climate change. Appl. Geochem. 25 (10), 1478–1486.
Wang, Y.-H., Yang, H., Chen, X., Zhang, J.-X., Ou, J., Xie, B., Huang, C.-C., 2013. Molecular biomarkers for sources of organic matter in lacustrine sediments in a subtropical lake in China. Environ. Pollut. 176, 284–291.
Wang, M., Wang, C., Hu, X., Zhang, H., He, S., Lv, S., 2015. Distributions and sources of petroleum, aliphatic hydrocarbons and polycyclic aromatic hydrocarbons (PAHs) in surface sediments from Bohai Bay and its adjacent river, China. Mar. Pollut. Bull. 90 (1–2), 88–94.
Wentzel, A., Ellingsen, T.E., Kotlar, H.K., Zotchev, S.B., Throne-Holst, M., 2007. Bacterial metabolism of long-chain n-alkanes. Appl. Microbiol. Biotechnol. 76 (6), 1209–1221.
Wiesenberg, G.L.B., Schwarzbauer, J., Schmidt, M.W.I., Schwark, L., 2004. Source and turnover of organic matter in agricultural soils derived from n-alkane/n-carboxylic acid compositions and C-isotope signatures. Org. Geochem. 35 (11−12), 1371–1393.
Wilhelms, A., Larter, S.R., Hall, K., 1994. A comparative study of the stable carbon isotopic composition of crude oil alkanes and associated crude oil asphaltene pyrolysate alkanes. Org. Geochem. 21 (6–7), 751–760.
Wise, S.A., Benner, B.A., Byrd, G.D., Chesler, S.N., Rebbert, R.E., Schantz, M.M., 1988. Determination of polycyclic aromatic hydrocarbons in a coal tar standard reference material. Anal. Chem. 60 (9), 887–894.
Xu, J., Lyu, H., Xu, X., Li, Y., Li, Z., Lei, S., Bi, S., Mu, M., Du, C., Zeng, S., 2019. Dual stable isotope tracing the source and composition of POM during algae blooms in a large and shallow eutrophic lake: all contributions from algae? Ecol. Indic. 102, 599–607.
Yoo, H., Kannan, K., Seong, K.K., Kyu, T.L., Newsted, J.L., Giesy, J.P., 2008. Perfluoroalkyl acids in the egg yolk of birds from Lake Shihwa, Korea. Environ. Sci. Technol. 42 (15), 5821–5827.
Yunker, Mark B., Macdonald, R.W., Vingarzan, R., Mitchell, R.H., Goyette, D., Sylvestre, S., 2002. PAHs in the Fraser River basin: a critical appraisal of PAH ratios as indicators of PAH source and composition. Org. Geochem. 33 (4), 489–515.
Zaghden, H., Tedetti, M., Sayadi, S., Serbaji, M.M., Elleuch, B., Saliot, A., 2017. Origin and distribution of hydrocarbons and organic matter in the surficial sediments of the Sfax-Kerkennah channel (Tunisia, Southern Mediterranean Sea). Mar. Pollut. Bull. 117 (1–2), 414–428.
Zhang, Y., Yu, J., Su, Y., Du, Y., Liu, Z., 2019. Long-term changes of water quality in aquaculture-dominated lakes as revealed by sediment geochemical records in Lake Taibai (Eastern China). Chemosphere 235, 297–307.
Zhang, Y., Fu, H., Liao, H., Chen, H., Liu, Z., 2022. Geochemical records of Lake Erhai (South-Western China) reveal the anthropogenically-induced intensification of hypolimnetic anoxia in monomictic lakes. Environ. Pollut. 299, 118909.
Zhang, Y., Fu, H., Yang, X., Liu, Z., 2023. Anthropogenically driven changes to organic matter input in sediments of Lake Chaohu, Eastern China, over the past 166 years. CATENA 231, 107285.